UiT The Arctic University of Norway

Faculty of Science and Technology
Department of Physics and Technology

Optimal sizing and placement of Electrical Vehicle charging stations to serve Battery Electric Trucks

With impacts on the Norwegian power system

Ole-André Isaksen

EOM-3901 Master's thesis in Energy, Climate and Environment - June 2023

“Someone is sitting in the shade today because someone planted a tree a long time ago.”

–Warren Edward Buffett

Abstract

For Norway to reach the emission limits in the Paris Agreement, a substantial amount of CO2 must be reduced. Road traffic alone accounts for a high percentage of the total emissions during 2021. This thesis will focus on electrifying the transport sector and analyzing charging infrastructure for heavy-duty electric vehicles. New charging infrastructure for heavy-duty Electric Vehicles (EVs) provides issues regarding profitability due to the currently low adaption rates. However, heavy-duty EVs use the same charging sockets as EVs. As a result, EVs may finance the charging infrastructure needed to increase the adaption of heavy-duty EVs. Projections from Norwegian grid operators suggest that the total electricity surplus is diminishing during the next years and will be negative by 2027. This highlights the importance of modeling the power system in combination with finding optimal locations for charging stations. This study uses prescriptive analytics to suggest optimal locations for charging infrastructure to maximize returned profits to motivate station builders to implement more charging stations. A soft-linking will be done with PyPSA-eur to model the power system, where the new infrastructure is added as an additional load. Analyzing the results, it is possible to see that charging infrastructure has the potential to become profitable as the adaption rate for heavy-duty EVs rise. The collaboration between the models offers an open-source tool for scholars, researchers, and planners to study how new charging infrastructure affects key components in the Norwegian power system and could be useful in modeling state-of-the-art technologies.

Acknowledgements

I am deeply grateful to my supervisor and co-supervisor, Chiara Bordin and Sambeet Mishra for their invaluable guidance, expertise, and insightful feedback throughout this study.

I would like to express my gratitude towards the prior work done in the field of prescriptive analytics, the musk-model, and the authors of PyPSA, along with everyone concerned in providing free data for academic purposes.

Special thanks to my office colleagues for their moral support throughout the thesis.

I would also like to thank my friends for reminding me of the important things in life, mainly all the fishing trips I have missed.

I am particularly grateful for my family who provided me with the best possible childhood, constant encouragement, and support throughout this journey.

Finally, I would like to thank Sofie for supporting me through thick and thin, and always being there for me.

Contents

List of Figures

1 Introduction

Political and economic instruments have caused an enormous increase in sales of new electrical vehicles (EV) in Norway, with a growth rate of 611% from 2016 to 2022, including all types of vehicles [1]. This has resulted in a substantial increase of EVs in the total car fleet. As a result of this growth, massive investments have been made to install chargers along the largest roadways in Norway.

Transport is one of the sectors in Norway with the highest emission of CO2, where road traffic alone accounts for 21% of the total emissions in Norway [2]. This shows the potential of reducing emissions by electrifying the transport sector. Several state-owned enterprises are driven towards operating with zero emissions due to governmental policies. One of the biggest contributors to this shift is the Norwegian mail services, Posten and Bring. They represent critical infrastructure and have the largest vehicle fleet in Norway. In 2025 they have an ambition to only use sustainable energy in vehicles and buildings [3]. They already utilize battery-electric vans and trucks. The latter brings interesting and problematic issues regarding the established charging infrastructure.

According to projections by *Statnett*, the power surplus of 5-7 TWh in Northern Norway is predicted to be negative by 2027 under a basic scenario [4]. Furthermore, the high-growth scenario projects a regional power deficit as early as 2026. This surge in electricity demand is primarily due to the electrification of heavy industries, petroleum activities, transportation, and the establishment of new green initiatives.

LKAB, Europe's largest iron ore producer, based in Kiruna and Malmberget, plans to eliminate CO2 emissions from its processes and production by 2045, requiring significant amounts of renewable energy. By 2030, LKAB will need 20 TWh of power, which will increase to 50 TWh by 2040 [5], equivalent to around 30% of Norway's typical annual electricity production.

Since the power grid in Northern Norway is more connected to Northern Sweden than Southern Norway, power deficits in both regions are expected to result in substantially higher electricity prices. To stay ahead of the projected power shortfall, exploring opportunities for new power production early on is crucial, as developing new facilities is time-consuming. Initiation of such projects now is necessary to ensure they can deliver electricity to the grid by 2030.

As Northern Norway approaches an energy deficit, the industry must expand and upgrade the current grid to ensure energy security. The cost of investing in grid expansion is very high. In the years up to 2030, *Statnett* plans to invest NOK 60-100 billion to reinforce the central grid [6]. To reach the emission objectives in the Paris Agreement, further research into charging site placement and its impact on the power grid is necessary.

1.1 Motivation

During an earlier project with Posten, they drove a battery electric truck (BET) from Oslo to Tromsø to evaluate the charging infrastructure for BETs. The main finding was that existing charging infrastructure was not facilitated for BETs, as they suspected. The vehicle used was a full-battery electric Scania P25, with a battery capacity of 300 kWh and a stated driving range of 250 km. Due to the large battery pack, most chargers were unusable, as the BET requires a voltage input of above 500V DC. Otherwise, the charging would fail even if the charging power were high. This resulted in two charging options: public rapid chargers (150-350 kW) with a sufficient output voltage above 500V DC. The second option was charging at 400V AC grids using a private mobile converter and transformer. For the latter, patience was required as the power output was 25 kW, resulting in a substantially longer charging time.

For further electrification of the vehicle sector: implementation, placement, and dimensioning of charging infrastructure for heavy-duty EVs will be crucial. Rapid chargers with sufficient voltage output are already implemented along several main roads in South Norway. On the contrary, few exist in Northern Norway. Therefore, establishing applicable infrastructure that can be utilized by both EVs and heavy-duty EVs in Northern Norway is an interesting case to study.

1.2 Hypothesis

This study aims to identify key aspects of optimizing the allocation and location of new rapid chargers intended for heavy-duty EVs. To achieve a better understanding of this study, relevant literature is reviewed to select models and methodologies that can be used to achieve the desired results. Background theory will be presented to help understand and implement methodologies and models. The objective function of the selected model is set to allocate the new rapid charging stations to areas with the highest demand. The most suitable locations are selected based on the most profitable locations to motivate station builders to implement more charging sites. The next part will analyze the strain of new chargers on the Norwegian power system. Based on general assumptions, it is predicted that the profitability of charging infrastructure for heavy-duty EVs is low due to the low adaption rate of these vehicles. If the adaption rate is instead projected for the currently existing EV fleet in Norway, then the project could prove to be profitable, meaning that the already existing EV fleet could finance charging sites later utilized by heavy-duty EVs. If the current and new chargers are implemented in the Norwegian power system, then the system cost is expected to rise substantially due to the capacity expansion of the power system. A GitHub repository is created for falsifiability, containing data sets and scripts for creating and analyzing the results, found at *github.com/o2i/Masters-Thesis* [7].

1.3 Contribution

This thesis broadly contributes to the research field of prescriptive analytics, with a focus on mathematical optimization applied to the field of EVs, optimizing charging stations for Heavy-duty electric vehicles with impacts on the Norwegian power system. The contribution is methodological and analytical. On the methodological side new modeling features will be built on top of an existing open-source model to tailor the tools to the specific problem at hand, involving heavy-duty EV infrastructures. Another methodological contribution is the soft-linking between two models that were built for different purposes. Linking the model for allocating optimal locations to the model that optimizes the grid results in a new purpose for the combined models, understanding the impact of higher penetration of EVs in the northern Norway power grid. Where the output of the allocation-location model becomes the input for analyzing the grid. The third methodological contribution is data gathering for real-world data. Consisting of dialog with industries, identifying industrial needs, data needs, and data manipulation to run and connect the models. The analytical contribution is double. The optimal location and sizing of the new charging infrastructure will be investigated in Northern Norway using real-world data and analyzing the impact of new loads in the power system.

2

Literature review

Since optimization and model building concerning EV charging stations and power systems is complex and interdisciplinary, the first part of this literature review aims to review literature related to EVs, charging infrastructure, and EV battery technology. The second part concerns optimization methods related to charging stations found in the literature, which can be divided into three main groups: design, operation, and location-allocation. With the main focus on the latter. The last part identifies literature on open-source power and energy system models.

In [8], the first experiments with EV are reviewed in early 1800 to early 1900. Due to discoveries made by Alessandro Volta (1745-1827) and Michael Faraday (1791-1867), who invented the electrical battery and the concept of a motor capable of rotating continuously. It led to a period known as the age of invention, with the electric motor being one of its most notable applications, including electric vehicles. While several theories, rumors, and viewpoints surround the initial electric vehicle, this text aims to identify the experiment that rightly deserves the title of the first-ever electric vehicle test. The discussion centers around the world's first electric vehicle. In [9], early applications of EV, early charging methods, and arguably the first public charging station are reviewed. It also highlights that EVs are not a new invention since they were utilized before vehicles with internal combustion engines.

A state-of-the-art review of charging station technology is proposed in [10]. Charging power levels, connectors, types, infrastructure, impacts, and standards are reviewed, along with an introduction to optimization methods for slow and rapid EV charging stations.

This article [11] presents an overview of electric vehicles and the different design aspects of charging stations. The charging stations are classified based on the power used, and various optimization algorithms and methods are discussed to achieve optimal design. The paper also highlights the combination of renewable energy-based and grid-connected systems, including their off-grid mode. Finally, the future directions and scope of this field are summarized.

The primary factors and obstacles that influence the widespread adoption of EVs are presented in [12]. Examining crucial aspects of EV technology, including the power levels of charging infrastructure, types of plugs, prevalent powertrain designs, and existing energy storage options. Additionally, the controllability of EV charging is briefly explored, highlighting its advantages for distribution grid management and its role in promoting the growth of renewable energy sources.

The energy demands necessary to meet the charging needs of EVs and evaluates the effect of EV demand on daily and annual system load profiles, proposed in [13]. Provides a detailed presentation of the deterministic and stochastic parameters that define the extra EV demand. The influence of this additional charging demand on the system load curve is examined for five European countries, including the United Kingdom, Germany, Spain, Portugal, and Greece.

EV battery technologies are introduced in [14]. Concerning the power and energy of electric propulsion systems. Introducing commonly used terminology for describing battery performance and characterization, then analyzing various battery charging techniques and EV charging strategies. The essentials of EV battery technologies are addressed, focusing on the two most prevalent types: Nickel Metal Hydride (NiMH) and Lithium-ion (Li-ion). Battery modeling and characterization are presented, covering aspects such as model parameter estimation, State of Charge (SOC), and State of Health (SOH) estimation. The integration of batteries for power grid applications is explored. The concept of a Virtual Power Plant (VPP) for battery aggregation is introduced to facilitate EV participation in power markets.

Numerous studies have focused on prevalent Li-ion technologies, which are now approaching their theoretical boundaries. Consequently, contemporary research is investigating potential successors, such as Lithium-Sulfur (Li-S) technologies. The authors of [15] evaluate and debate different battery modeling methodologies, encompassing mathematical models, electrochemical models, and electrical equivalent circuit models. Following a broad overview, the research delves into the particular utilization of battery models within electric vehicle battery management systems. Models may possess lower fidelity to ensure rapid execution in real-time applications.

A comprehensive examination of new technologies in the transportation industry, evaluating eco-friendly chemical processes as innovative green energy sources for electric vehicles and portable power in the microelectronics domain, is proposed in [16]. Moreover, this investigation explores and assesses the potential advancements of biological systems in energy generation, considering the perspective of bio-batteries.

An introduction to model building in mathematical programming can be found in [17]. This book is intended to provide students with a solid foundation in the principles of model building, including the mathematical and algorithmic aspects of the subject.

A systematic reference for grid scheduling considering intelligent electric vehicle integration can be found in [18]. The authors discuss state-of-the-art scheduling techniques for incorporating plug-in EVs, a thorough analysis of traditional analytical scheduling, and optimizing techniques like game theory, meta-heuristic algorithms like the genetic algorithm, linear, non-linear mixed integer programming, and dynamic programming.

An approach for the design of Heavy-Duty Electrical Vehicle (HDEV) charging stations is proposed in [19]. In order to find Pareto optimal designs, this paper introduces a bi-level multi-objective optimization framework, with realistic power loss models and optimally sized power electronic converters as constraints. This bi-level approach simplifies the design process by dividing charging station optimization into a system-level problem and multiple converter-level problems. The effectiveness of this approach is demonstrated for a 9-port charging station, using industry-based HDEV arrival times and charging conditions.

In [20], a comprehensive review of the literature about charging station location problems concentrates on problem modeling and resolution. Reviewing the literature from various angles, encompassing demand representation, demand coverage strategies, objective functions, side constraints, decision variables, model structure, and the influence of time dependency and uncertainty on problem parameters.

A comparative analysis of charging station allocation-location in academic research compared to the actual practice of charging station placement is described in [21]. The author intends to emphasize the gap between academic research and charging station placement strategies utilized in practice.

In [22], an uncapacitated gradual maximal covering model approach is proposed for determining the optimal locations of BEV charging stations in urban environments. This method thoroughly examines BEV charging requirements, coverage, and potential for adoption, in conjunction with a novel location-allocation model. The applicability of this approach is showcased through a series of hypothetical scenarios that emulate the elements of real-world charging station location challenges.

The return on investment for electric vehicle charging stations and presents a Mixed Integer Linear Programming (MILP) model integrated with Geographic Information System (GIS) for pinpointing optimal charging station locations in urban areas, is proposed in [23]. The efficacy of the proposed methodology is illustrated through a case study conducted in Västerås, a city in central Sweden.

An optimization model for strategically placing charging stations to minimize overall costs while ensuring charging reliability and maintaining the expected quality of service for EV owners and drivers is proposed in [24].

The authors of [25] propose two distinct optimization models to identify the optimal locations for public charging stations, considering two different charging modes, fast and slow charging. They use a framework for geographic segmentation (GS) compared to a complementary partial (CP) coverage approach.

A GIS-based Multiple-Criteria Decision Analysis (MCDA) approach to handle the problem of EV charging site selection is proposed in [26]. They utilize the fuzzy Analytical Hierarchy Process (AHP) and Technique for Order Preference by Similarity to Ideal Solution (TOPSIS) to identify the best EV charging site locations. This hybrid method is applied as a case study in Ankara, Turkey. The findings indicate that the proposed alternative sites surpass the existing 12 EV charging site locations in terms of the evaluated criteria.

Elementary features of Python for Power System Analysis (PyPSA) is presented in [27]. It is based on the full power flow equations formulation and multi-period optimization of operation and investment using linear power flow equations. Serving as a bridge between traditional steady-state power flow analysis tools and comprehensive multi-period energy system models within free, open-source software. Models for traditional power plants with unit commitment, variable renewable energy generation, storage facilities, connections to other energy sectors, and mixed AC and DC networks are all included. PyPSA is intended to be easily extensible and scalable for large networks and extended time series. The authors compare PyPSA with other free and paid software regarding energy and power system modeling. A comparison is made between PyPSA and other free software: MATPOWER [28], pandapower [29], PSAT[30], PYPOWER [31], calliope [32], minipower [33], MOST [34], oemof [35], OSeMOSYS [36], PowerGAMA [37], urbs [38].

PyPSA-Eur (Python for Power System Analysis - Europe) is presented in [39], introducing the first open model dataset of the European power system at the transmission level. The model can be used to plan operational, generational, and transmission expansion studies. Due to its continental scope and highly resolved spatial scale, it is possible to accurately depict the long-range smoothing effects of renewable energy generation and their fluctuating resource availability.

In light of this review, optimizing EV charging stations is important in the field to optimize location and allocation to optimize resources and maximize the utility of charging infrastructure. Norway is interesting to study due to the high adaption rate of EVs and its ambitious goals for reducing internal combustion vehicles. Many self-contained models exist in literature focusing on specific aspects of charging stations and power grids. Still, there is a gap between more holistic models that link EV decision-making with power systems decision-making aspects. This motivates the idea of exploring the development of such links, as done in the thesis.

3
Background

Prescriptive analytics involves using decision models, including optimization models, in managerial decision-making. It is the final and most advanced category. Prescriptive analytics involves using decision models to prescribe what should be done in the future [40]. It exceeds descriptive, diagnostic, and predictive analytics when considering value against difficulty, as proposed by Gartner [41]. This thesis will focus on the optimization part of prescriptive analytics. The main objective of this section is to provide the reader with an introduction to key concepts of mathematical optimization and the models used in the thesis.

3.1 Mathematical optimization

It is a method used to find optimal or near-optimal solutions to a given problem. In optimization, the objective is to maximize or minimize a specific problem. The object to be maximized or minimized is called an objective function. That is subject to a set of constraints for determining the desired variables in the objective function. Together the objective function and the constraints represent a mathematical model. That involves a number of mathematical connections, including equations, inequalities, and logical dependencies. They frequently correspond to practical relationships found in the real world, such as those found in technology, physical laws, and marketing constraints. [17].

A simple analogy for mathematical optimization could be to visualize the model as an arcade game, where the objective could be to get the highest score (maximize) or to complete the game in the shortest amount of time (minimize) by following the rules of the game (constraints).

The term mathematical programming is often confused with computational programming [17]. Mathematical programming differs from computational programming as the programming term refers to "planning". Therefore, it does not have to involve computers. The two interconnect when involving practical problems with a large amount of data present, then it is only reasonable to handle the problem using computing power.

Mathematical optimization is interdisciplinary and usually requires knowledge in multiple fields, like mathematics, physics, economics, logistics, and more. It is one of the most used tools in operational research and management science. For instance, a problem could be to determine the maximum profit of a mix of products at a factory with limitations on resources and production capacity.

The most common programming models can be categorized into: Linear Programming (LP), Integer Programming (IP), Non-linear models, and Quadratic Programming (QP). Multiple sub-categories can present each category. This thesis will mostly focus on LP and Mixed Linear Integer Programming (MILP) problems.

3.1.1 The role of mathematical optimization in renewable energy

Mathematical optimization is not a new phenomenon in renewable energy. It plays a significant role in the planning, designing, and operating of renewable energy systems. Mathematical optimization help to address different problems and make data-driven, optimal decisions, like improving efficiency and reliability or reducing costs, maximizing profits for renewable energy systems. For instance, mathematical optimization could identify the optimal location for new energy systems, like solar or wind installations. Considering aspects such as wind speeds, land-use classification or availability, solar irradiance, etc. The objective function could be to maximize energy production while minimizing costs and environmental impact. There are a ton of other applications of mathematical programming in renewable energy systems. To summarize, mathematical optimization is invaluable in the planning, designing, and operating of renewable energy systems.

3.1.2 Linear Programming

For a model to be linear, it requires both the objective function and constraints to be linear expressions. If it contains expressions like $3x^2$, e^x, $\frac{1}{x}$, etc, then it is not a linear expression. For a model to be linear, it must include expressions like $7+2x$, $5x+x$, $\frac{1}{3}x+3x+5$, etc. LP is given much attention due to being easy to solve compared to non-linear models. Not everyone has access to expensive computers with great computational power. However, it is important only to implement LP where it represents a valid or approximately valid model.

3.1.3 Simplex algorithm

The simplex algorithm is the most widely used method for finding an optimal solution to linear programming problems. It was originally developed by the American mathematician George Dantzig in 1947 to solve linear programs for planning and decision-making in large-scale enterprises [42]. Multiple enhancements and advancements have been made since then to improve the algorithm. The approach is rooted in searching for the minimum value among the vertices of a polyhedron defined by constraints. The process begins with selecting one of the vertices and then directing the search toward the first vertex where the objective function shows a decrease. If no such vertex exists, then the current vertex represents the minimum. However, if there is a vertex where the objective function decreases, the current vertex becomes the starting point for a new search. [43]. Ultimately obtaining the optimal solution. Because the simplex algorithm only looks at vertex solutions, rather than the typically infinite set of impossible solutions, linear problems are simple to solve. Even in a scenario where alternate solutions exist, there will always be an optimal solution that lies at a vertex [17].

3.1.4 Integer Programming

An IP model consists of integer (whole numbers) variables. It involves making decisions based on integers. It can be useful for certain goods and integral quantities of resources. For instance, goods or resources that would not make sense to have a decimal value, like employees, houses, lamps or planes. IP models offer wide applicability often referred to as *discrete programming* [17]. A model consisting of solely integer values is known as pure integer programming (PIP) model. More frequently, there are models with integer and conventional continuous variables. Such a model is a mixed integer programming (MIP) model [17]. However, IP models involve many times as much calculation and computational power compared to LP models. And most IP models can be solved using LP models and then rounding off the optimal solution to the closest integer. Practical IP models commonly represent boolean values as integers (0 and 1), meaning yes or no, to make decisions, also called Binary Integer Programming (BIP) [40].

3.1.5 Mixed Integer Linear Programming

Mixed Integer Linear Programming, hereby denoted as MILP, involves finding the optimal solution to a problem with a linear objective function, subject to constraints consisting of linear expressions and a set of decision variables represented by integers. It is a subcategory of MIP models. The linear continuous variables can take any value in a specified range, as it would if the problem were fully linear. At the same time, integers must represent the decision variables. The mix of linear and integer variables adds complexity to the solving process. Implementing special algorithms to find a solution may be necessary, as the integer constraints could make the problem non-convex. It is a powerful tool due to its modeling capability, but for large models, it suffers computationally and might be unsolvable.

3.1.6 Algorithms for solving IP problems

There is no single perfect algorithm for solving IP problems like there is for LP with the simplex algorithm. Different algorithms work better for different types of problems. It's unlikely that a universal IP algorithm will ever be discovered. If one were found, it could solve many complex problems. The branch and bound method is the most successful algorithm for solving general IP problems, according to [17]. Even though it seems simple, it works surprisingly well. Almost all commercial software packages that handle MIP use this method. The algorithm is very flexible and can be adapted to different problems. Using the branch and bound method smartly can lead to significant improvements. There are four main methods for solving IP problems, with some overlap. Some successful approaches to large problems have taken advantage of features from several methods.

Branch and Bound Since any bounded PIP problem has a finite number of feasible solutions, an enumerative approach is sensible to find an optimal solution. Unfortunately, the finite number is usually extremely large. Therefore, the enumerative process must be cleverly structured only to examine a fraction of the feasible solutions. The basic concept for the branch and bound method is to divide and conquer by dividing the problem into smaller and smaller subproblems until these subproblems can be conquered [40]. This algorithm has demonstrated the greatest success in tackling practical MIP problems. They are occasionally categorized as enumerative techniques. However, it is important to separate from the enumerative methods mentioned in the other algorithms. Like cutting plane methods, the IP problem is initially addressed as an LP problem by relaxing the integrality constraints. If the resulting solution is an integer, the problem is considered solved. If not, a tree search is conducted to explore feasible solutions and find the optimal integer solution. By integrating the tree search with other techniques, such as cutting planes, these hybrid methods can efficiently navigate the solution space and improve their effectiveness in solving a wide range of MIP problems [17].

Cutting plane While cutting plane methods might seem mathematically sophisticated, they have not successfully tackled large-scale problems. Nevertheless, they can become highly effective when combined with Branch and Bound techniques. The first method of this kind was introduced in [44] by Gomory in 1958. A cutting plane for any IP problem is a new constraint that reduces the feasible region without eliminating feasible solutions [40]. The algorithm can be utilized for general MIP problems. Typically, they begin by addressing an IP problem as if it were a LP problem, disregarding the integrality constraints (LP relaxation). The continuous LP solution that results will also function as an integer optimum if it is an integer. If it is not an integer, the problem is systematically further constrained by adding more restrictions or cutting planes. It's possible or unlikely that an integer will be the next solution to the more restricted problem. The IP problem can be solved by repeatedly performing this procedure until an integer solution is found or the problem is determined to be infeasible. [17]. Adding cutting plane to the branch and bound method can accelerate how quickly an optimal solution is found.

Enumerative These methods are typically employed for the distinct category of binary PIP problems. Theoretically, this category has a finite number of potential solutions for problems. Although analyzing all possibilities would be impractical, a tree search can examine a subset of solutions while systematically eliminating numerous others as infeasible or non-optimal. These techniques and their variations and expansions have proven highly successful for certain problem types while demonstrating limited success for others. Commercial software packages implementing these methods exist, but their usage is not widespread [17]. Enumerative methods have an advantage over branch and bound programming as they have the capability to preserve any unique structure that may exist in the problem. However, a drawback of enumeration methods is that they require resolving an integer program at each iteration, which can be computationally demanding. A more appealing approach appears to be integrating the concept of partitioning into an enumerative scheme, as it offers computational advantages [45].

Pseudo-Boolean Pseudo-boolean methods for solving optimization problems aim to find the optimal binary values that maximize or minimize a given objective function, usually by pseudo-boolean expressions. It has been tried to take advantage of the obvious similarity between binary PIP issues and boolean algebra. Many different algorithms have been created. They perform admirably on some problems but less so on others, similar to other algorithms. This method of resolving IP issues is completely distinct from all others. Boolean algebra is used to express constraints rather than equations or inequalities. In some instances, this can provide a clear overview of the constraints, but in others, it is large and impractical. [17].

3.1.7 Solvers

Open-source and commercial solvers are the two main tools for solving mathematical optimization problems. In the open-source category, tools like COIN-OR Linear Programming (CLP), GNU Linear Programming Kit (GLPK), and SCIP exist. CLP is a popular choice for solving linear and mixed-integer programming problems, while GLPK is another powerful tool that works well with large-scale problems. SCIP is a versatile solver that can handle various problems, including mixed-integer linear, nonlinear, and constraint integer programming.

As for commercial solvers, some of the most popular options are IBM ILOG CPLEX (CPLEX), Gurobi, and FICO Xpress. CPLEX is a top-performing solver that works with linear, mixed-integer, and quadratic programming problems. It's known for being fast, scalable, and reliable in solving complex industry problems. Gurobi is another widely-used solver with cutting-edge algorithms, making it highly efficient in solving linear, mixed-integer, and quadratic programming problems. Finally, FICO Xpress is an all-in-one optimization suite that can handle various problems, from small-scale to large, real-world applications. It also includes tools for modeling and analytics.

3.2 Different types of optimization

Optimization can be classified into three different types of optimization: heuristics, metaheuristics, and exact methods. This thesis utilizes exact methods for choosing the optimal location for EVs and for analyzing the impact of the new charging stations on the power system.

3.2.1 Exact methods

In optimization, exact methods ensure finding an optimal solution, searched using accurate, deterministic numerical algorithms. Typically, an exact optimization approach is preferred when it can address an optimization issue with an effort that increases polynomially with the problem size. However, for NP-hard problems, the situation changes, as exact optimization methods require exponential effort. As a result, even moderately-sized problem instances frequently become unmanageable, making it impossible to solve them using exact methods [46], resulting in having to use heuristics or a combination of exact methods and heuristics. This provides challenges for both models used in this thesis. For the optimal location model used in this thesis, the demand grid implementation has a huge impact on computational time and tractability. The computational time for the power system model can be reduced by aggregation techniques as explained in the PyPSA documentation [47] for instance changing the granularity of the problem.

Recently, engineering optimization practitioners have increasingly combined various optimization techniques to achieve more accurate solutions. The initial stage involves using reduced-complexity algorithms to generate moderately accurate solutions. In the second stage, these preliminary solutions are starting points for higher-accuracy algorithms. Integrating exact and meta/heuristic methods, often derived from evolutionary programming, is also feasible, particularly when the solution must meet additional constraints, such as having integer values or residing in discrete subspaces of the search area [43]. If the problem at hand is too big, complex, or computationally hard, heuristics or metaheuristics can be utilized to find good solutions that are not optimal.

3.2.2 Heuristics and Metaheuristics

Loosely defined, the term "heuristic" refers to finding or discovering through trial and error. These algorithms can find high-quality solutions to complex optimization problems in a reasonable time [48]. Heuristic techniques, also known as "search algorithms," are problem-solving approaches that involve exploring possible solutions for a given problem, known as the "search space." Unlike exhaustive search methods, heuristic techniques such as "evolutionary algorithms," "local search methods," and "simulated annealing" offer an alternative approach to solving challenging computational problems within a reasonable timeframe [49]. There is no assurance of reaching the optimal solution. Heuristic algorithms tend to work well most of the time, although not always. This characteristic is advantageous when the goal is to obtain good solutions that are easily attainable rather than necessarily the best [48].

Metaheuristic algorithms represent a further development of heuristic algorithms. The prefix "meta" denotes a higher level or going beyond. Generally, metaheuristic algorithms outperform simple heuristics. They rely on randomization and local search, with tradeoffs involved. It's important to note that there is no consensus on the exact definitions of heuristics and metaheuristics in the literature. Some researchers use these terms interchangeably, but the current trend refers to stochastic algorithms involving randomization and local search as metaheuristics [48]. Randomization allows for exploration on a global scale, moving away from a purely local search. Consequently, almost all metaheuristic algorithms are well-suited for global optimization.

3.2.3 Sensitivity Analysis

Sensitivity analysis can be utilized to explore uncertainty within deterministic models through so-called what-if-analysis. This study will exclusively focus on deterministic methodologies. This methodology can be further classified into two groups: those that explore local sensitivities, achieved by investigating the impact of minor modifications to the model parameters, and those that investigate global sensitivities, achieved by analyzing the model dynamics within a substantial parameter space. Sensitivity analysis has expanded over recent years, being utilized to analyze models across various scientific fields [50]. This thesis aims to analyze local sensitivities to explore how certain parameters affect the model's objective value.

3.3 Optimal location of EV charging sites

A MILP approach for finding the optimal location of charging sites using GIS is described in [23]. Based on this paper, Obed Sims contributed an open-source implementation on GitHub [51], Where he implements a case study based in Manchester, England. This model implementation is hereby referred to as musk-model, which will be further developed in the methodology section. The musk-model is selected because it handles the problem of interest (optimal location of charging stations) with the methodology of interest (optimization). The model is open-source, which accelerates the implementation of the mathematical model in [23]. Due to its user-friendly modeling structure, it represents a starting point for further development in terms of new functionalities and linking with other tools for power systems analyses. The musk-model states what type of data sets are used in the model, which makes it easier to identify similar data needed for a case study in Norway.

3.3.1 Mathematical model

The objective function (3.1) seeks to maximize the total profit of new charging stations. The variables to be maximized are x_j, a binary variable whether car park j is selected for a charging station, n_j, the number of chargers in station j, and q_j, the number of cars charged by station j. The decision variables in the model include x_j, n_j, and q_j, which will be decided when the model is solved.

$$MaximizeProfits\left(x_j, n_j, q_j\right) = \sum_{j=1}^{J} \left[p_j \cdot t_j \cdot q_j - c_j\right], \quad j = 1, 2, \ldots, J \quad (3.1)$$

Where p_j is the charging price per minute for station j, the estimated charging duration for an EV being fully charged is denoted by t_j, the charging demand covered by each station j is q_j, the total cost for each station is denoted by c_j.

Subject to,

$$q_j \leq n_j \cdot m_j \quad (3.2)$$

$$q_j \leq \sum_{i=1}^{I} r_{ij} \cdot dr_i \quad (3.3)$$

$$\sum_{j=1}^{J} x_j \cdot r_{ij} \leq 1 \quad (3.4)$$

$$n_j \geq x_j \quad (3.5)$$

$$n_j \leq l_j \cdot x_j \quad (3.6)$$

$$\sum_{j=1}^{J} x_j = N \quad (3.7)$$

$$x_j, n_j \geq 0, \text{ where } x_j \text{ and } n_j \text{ are integers}, \quad (3.8)$$
$$j = 1, 2, \ldots, J \text{ and } i = 1, 2, \ldots, I.$$

These constraints are implemented to ensure maximum profit for each charging station. Eq (3.2) is related to capacity, where n_j the number of cars charged by the station must be less or equal to n_j, the number of chargers in the station, multiplied by m_j, the maximum serving time of each charger per day.

Equation (3.3) is a constraint related to demand. The number of charged cars must be less or equal to the sum of r_{ij}, the demand coverage level of station j on demand node i, multiplied by dr_i, the remaining demands in cell i. Note that dr_i cannot be a negative number. Therefore, the minimum demand must be limited to zero.

Constraint (3.4) indicates that a single charging station can only serve the remaining demand in grid i, guaranteeing that distinct demand nodes are allocated to separate charging sites. Both x_j and r_j are binary values.

Equation (3.5) and (3.6) add a limitation for the number of charging points. The two constraints ensure that each station has at least one charger and, at most l_j charging points. If there is no charger, then the constraints imply that there is no charging point either. Constraint (3.7) ensures that a specific number N of new charging stations is installed. Finally, constraint (3.8) states that all decision variables should be integers and not negative.

3.3.2 Calculations

Before the problem can be solved, a few calculations are necessary to define some of the parameters in the mathematical model, see equations (3.9) - (3.10).

$$c_j = \left(c_j^r + c_j^e + c_j^i + O\&\mathrm{M}_{\mathrm{Cost}} \cdot \left(c_j^e + c_j^i\right)\right) \cdot n_j + p_e \cdot \alpha \cdot q_j, \tag{3.9}$$

Equation (3.9) calculates the total cost of constructing a single charging station. The expenses associated with a charging station include rent, equipment, installation, maintenance and operation, and electricity costs, which fluctuate depending on the quantity and kind of chargers. Rent costs for charger installation sites and parking spaces are determined by the opportunity cost of the parking lot, equivalent to the parking fees the owner would earn if the space were used for paid parking. Additionally, it is assumed that maintenance and operation expenses amount to 10% of the equipment and installation costs.

As mentioned, c_j is the total cost of each station. The number of charging points in each station is denoted by n_j. c_j^r is the parking fee per day for each station. c_j^e is the capital cost of acquiring each charging station, while c_j^i is the cost associated with installing each one. The price the station owner pays per kWh of electricity is denoted by p_e. The average capacity of EV batteries, in kWh, is assumed to be α. The number of EVs charged by a specific station or each station's remaining demand is denoted by qj.

The electric vehicle charging infrastructure in the city must be factored into the model, as it addresses a portion of the demand. Assume that there are Z charging stations installed within the district, and the remaining charging needs for cell i are:

$$dr_i = d_i - \sum_{z=1}^{Z} d_{iz}, z = \mathbb{N} \tag{3.10}$$

In this scenario, dr_i represents the unmet charging needs in cell i, while d_{iz} denotes the demand in cell i satisfied by the existing station z.

Maximizing profits relies heavily on charging demand, which is a crucial variable. The entire study area is divided into uniform small grids, with their centroids serving as demand nodes. Further details regarding grid partitioning can be found in [24]. It is also assumed that the anticipated EV adoption rate in traffic flow is represented by v_0, while v_i refers to the charging possibility in grid cell i. A charging possibility, u, is defined to illustrate the varying charging opportunities for electric vehicles across different grids. In (3.11), d_i signifies EV charging demand in grid i and refers to the average traffic flow within grid i.

$$d_i = u \cdot v_i \cdot f_i \tag{3.11}$$

In (3.12), x_j represents a binary decision variable for whether car park j is selected for a charging station.

$$x_j = \begin{cases} 1, & \text{if there already is a station in parking lot j.} \\ 0, & \text{otherwise.} \end{cases} \tag{3.12}$$

In (3.13), r_j^i is the demand coverage level of station j on demand node i, while s_{ij} is the distance between station and demand node. The idea of a service area is based on the assumption that a charging station can only cater to the traffic flow within a specific region. The service radius of a station is set to L meters, which is comparable to the length of the grid i. A binary variable, r_j^i, represents the coverage level of station j on demand node i. If demand node i is covered by station j, r_j^i is 1. Otherwise, it is 0.

$$r_j^i = \begin{cases} 1, & s_{ij} \leq L. \\ 0, & s_{ij} > L. \end{cases} \tag{3.13}$$

Maximizing overall profits greatly depends on the optimal locations of charging stations, which are significantly influenced by the distribution and quantity of charging demands. This model determines charging demands based on daily traffic flow at various measurement points. However, these measurement points may not be uniformly distributed or absent in some areas. To effectively utilize the traffic flow data, a grid network is established. The target district is divided into i uniform small grids, each with a side length of L meters. The centroids of these grids serve as demand nodes, where the average traffic flow fi in grid i can be calculated using (3.14). Where K_i is the total number of traffic flow measurement points. f_{k_i} represents the daily traffic flow at measurement point K_i. For grids without any measurement points, the traffic flow is determined by averaging the values from surrounding grids.

$$f_i = 1/K_i \sum_{k_i=1}^{K_i} f_{k_i} \tag{3.14}$$

The charging possibility of an EV v_i is explained in equation (3.15). Here, various land-use classifications, such as residential with villas, residential with apartments, working, commercial, mixed land-use, and other areas, are identified using GIS to diversify charger types and charging possibilities for EVs in different locations. Fast chargers are assumed to be installed in commercial or mixed-use areas, while slow chargers are allocated to working or apartment areas. Moreover, in districts where people are more likely to stop and stay, such as commercial, working, and residential areas (excluding residential areas with villas since residents typically have home chargers), the charging possibility for an EV is set at v_0. Conversely, in areas where people seldom linger, like forests or farmlands, the charging possibility is 0. As multiple land-use types can be found within a single grid, the overall charging possibility in each cell must be calculated based on the area of each land-use type.

$$v_i = A_i/A \cdot v_0 \tag{3.15}$$

Where A_i is the sum of the different land-use classifications in grid i where it is satisfactory to install new charging stations, and A is the total area of grid cell i.

3.4 Power system modeling

Detailed physical modeling must be secondary to algorithmic feasibility in the context of large-scale optimization. This implies sacrificing numerous important details for power systems to achieve models compatible with previously discussed algorithms for solving optimization models [52]. An important question to ask is, why focus on power? When voltage and current have a much simpler relationship through Ohm and Kirchhoff's laws compared to power's quadratic dependence on voltage. The reason is that voltage or current alone is not practical. Loads require power for tasks like lighting, temperature control, and manufacturing. As a result, specifying a load in terms of voltage necessitates making assumptions about current and vice versa, determining their power need. Similarly, power plants consume fuel or harness energy from sources like water, wind, and sunlight, and their primary compensation is based on the power they generate. Consequently, modeling power systems in terms of power is an unavoidable aspect of power system engineering [52].

3.4.1 Linearized power flow

Linearized power flow refers to approximating and simplifying power flow equations. It can be obtained from the following four approximations: All voltage magnitudes are close to one per unit $|v_i| = 1$. Conductances are negligible compared to susceptances $g_{ij} \ll b_{ij} \implies g_{ij} = 0$. The nearly linear regions are occupied by voltage angle differences that are small enough be occupy this region, which means that $sin(\theta_i - \theta_j)$ is replaced by $\theta_i - \theta_j$. Relative to real power flows, reactive power flows are negligible, meaning all reactive power variables and constraints are removed [52]. Ultimately, obtaining the following linear feasible set of power flow:

$$p_{ij} = b_{ij}(\theta_i - \theta_j) \tag{3.16}$$

$$\sum_j p_{ij} = p_i \tag{3.17}$$

$$\underline{p}_i \leq p_i \leq \bar{p}_i \tag{3.18}$$

$$|p_{ij}| \leq \underline{p}_{ij} \tag{3.19}$$

Ohm's law arises when voltage angles are considered real voltages, susceptance is interpreted as the reciprocal of resistance, and real power is associated with current. Consequently, the simplified power flow model is often known as "DC power flow" [52]. A linear approximation of power flow equations makes optimization models more easily solvable, which is crucial in power system modeling.

3.5 PyPSA

PyPSA stands for Python for Power System Analysis. It is a free software toolbox for simulating and optimizing modern electrical power systems. Due to the increasing electrification of all energy demand, and fluctuating energy sources from renewables, the importance of software modeling has risen [27]. This introduces new challenges to the generation side, where variable renewable generation causes loads in parts of the grid that were never expected. This introduces new stochastic influences on flow patterns.

PyPSA represents the power system by the following components: network, sub-network, buses, generators, lines, line types, transformers, transformer types, carriers, links, loads, storage units, stores, shunt impedance, and global constraints (for adding a limit to CO2 emissions) [27], [53]. The network component is the overall placeholder for all the other components. Sub-network contains a sub-set of buses and passive branches. Buses act as an electrically fundamental node that connects components. They have a mathematical role in enforcing energy conservation by Kirchoff's current law. Generators connect to a single bus and feed power into the system. Lines represent transmission and distribution lines, that connect between two buses. Line types represent the standard line type per length values for impedances. Transformers represent 2-winding transformers used to change the voltage layer of AC power. Transformer types are a table with different standards for transformers. Carriers represent energy carriers, for instance, solar or onshore wind. Loads consume reactive and active power from the energy system and connect to a single bus. A single bus connects storage units, which are used for intertemporal power shifting. Independently of the storage power capacity, the storage energy capacity can be optimized using the store components. Shunt impedances connect to a single bus and have a voltage-dependent admittance. Global constraints are applied to many components at once.

PyPSA uses linear power flow equations to calculate the optimal power flow to minimize the total annualized system costs. A power system for a 24-hour resolution network can be modeled by the following set of objective function and constraints [27], [54]:

3.5.1 Objective function

$$\min_{g_{i,s,t};f_{\ell,t};g_{i,r,t,\text{charge}};g_{i,r,t,\text{discharge}};e_{i,r,t}} \sum_{s} o_s \cdot g_{i,s,t} \tag{3.20}$$

3.5.2 Constraints

$$0 \leq g_{i,s,t} \leq \hat{g}_{i,s,t} \cdot G_{i,s} \tag{3.21}$$

$$-F_\ell \leq f_{\ell,t} \leq F_\ell \tag{3.22}$$

$$d_{i,t} = \sum_s g_{i,s,t} + \sum_r g_{i,r,t,\text{discharge}} - \sum_r g_{i,r,t,\text{charge}} - \sum_\ell K_{i\ell} \cdot f_{\ell,t} \tag{3.23}$$

$$0 = \sum_\ell C_{\ell c} \cdot x_\ell f_{\ell,t} \tag{3.24}$$

$$0 \leq g_{i,r,t,\text{discharge}} \leq G_{i,r,\text{discharge}} \tag{3.25}$$

$$0 \leq g_{i,r,t,\text{charge}} \leq G_{i,r,\text{charge}} \tag{3.26}$$

$$0 \leq e_{i,r,t} \leq E_{i,r} \tag{3.27}$$

$$e_{i,r,t} = \eta^0_{i,r,t} \cdot e_{i,r,t-1} + \eta^1_{i,r,t} \cdot g_{i,r,t,\text{charge}} - \frac{1}{\eta^2_{i,r,t}} \cdot g_{i,r,t,\text{discharge}} \tag{3.28}$$

$$e_{i,r,0} = e_{i,r,|T|-1} \tag{3.29}$$

With the following parameters: $o_{i,s}$ is the marginal generation cost of technology r at bus i, x_ℓ is the reactance of transmission line l, $K_{i\ell}$ is the incidence matrix, $C_{\ell c}$ is the cycle matrix, $G_{i,s}$ is the nominal capacity of the generator of technology s at bus i, F_ℓ is the rating of the transmission line l, $E_{i,r}$ is the energy capacity of storage r at bus i, $\eta^{0/1/2}_{i,r,t}$ denote the standing (0), charging (1), and discharging (2) efficiencies.

The model has the following decision variables: $g_{i,s,t}$ is the generator dispatch at bus i, technology s, time step t, $f_{\ell,t}$ is the power flow in line l, $g_{i,r,t,\text{dis-/charge}}$ denotes the charge and discharge of storage unit r, at bus i and time step t, $e_{i,r,t}$ is the state of charge of storage r at bus i and time step t.

The first constraint Eq (3.21), is to ensure that the generators in the power system are not exceeding its capacity limits. Eq (3.22) ensures that the power system's transmission lines are within capacity limits. Eq (3.23) guarantees that the inelastic electricity demand $d_{i,t}$ at every bus n should be satisfied at each time t through a combination of local generators, storage, or the incoming flows f_t from the branches. Eq (3.24) ensures the physical integrity of the network flows, the application of Kirchhoff's Voltage Law is necessary in addition to Kirchhoff's Current Law. Kirchoff's Voltage law asserts that the sum of voltage differences around any closed cycle in the network must be zero. Expressing each independent cycle c as a directed combination of passive branches using a matrix C_{lc}. The constraint for ensuring discharge limits in storage units is implemented in Eq (3.25), while Eq (3.26) constrains the charging limits of storage units. Eq (3.27) puts a constraint on the energy capacity limits of storage units by having to be consistent between all hours, where Eq (3.28) relate the consistency of the storage units, and Eq (3.29) relate to the cyclicity of the storage units. Additional constraints can be added to the model to account for CO2 emission limits, sector-coupling, unit commitment, and more.

3.6 PyPSA-eur

It is the first open model dataset of the European power system to cover the full ENTSO-E area. The dataset consists of 6001 lines, including all high voltage direct current lines and alternating current lines with a voltage level of 220 kV or higher. Additionally, it has 3657 substations, a recently released open database of conventional power plants, time series data on electrical demand and the availability of variable renewable generators, as well as geographic analyses of the potential for expanding wind and solar power [39]. It consists of multiple scripts that add data to the network components in PyPSA. It utilizes *snakemake* to manage the workflows and run multiple scripts in parallel. It is possible to conduct an electricity-only or sector-coupled study that was recently added to PyPSA-eur, depreciating the model PyPSA-eur-sec. It contains a configuration file *config.yaml* where different parameters can be adjusted. For instance, which carriers to include in the model or building a model for a single country or multiple countries. Increasing the number of countries in to model also increases the problem at hand, making it more computer heavy to solve. According to Tom Brown (one of the authors of PyPSA), using Gurobi with PyPSA-eur-sec with the original settings in *default.config.yaml* a model with 181 nodes and 3-hour resolution can be solved in 6-8 hours with 100 GB of RAM [55]. The computer used in this thesis is installed with 16 GB of RAM. Therefore an electricity-only study was selected.

PyPSA-eur can be installed from the GitHub repository in [56]. A comprehensive introduction to using PyPSA-eur is found at [47]. When PyPSA is pulled from GitHub, the environment is installed and activated, and the configuration file is correctly set up, PyPSA-eur is ready to use. When PyPSA-eur is running, it first creates a base network containing high-voltage AC and DC lines before creating the electricity network, the network is then simplified and clustered into a selected number of nodes. The network can then be solved using the PyPSA package. This process can also be run step by step and will be key to implementing custom components to the power system model.

3.6.1 Nearest neighbour algorithm

An algorithm for finding the nearest neighbor is described in[57], which is the foundation for the python method *scipy.spatial.KDTree* found in the *SciPy* user manual [58]. It describes the k dimensional-tree as a binary tree, with each node representing an axis-aligned hyperrectangle. Every node identifies an axis and partitions the set of points according to whether their coordinate along that axis is greater or smaller than a specific value. The "sliding midpoint" rule is employed during construction to select the axis and splitting point, which prevents the cells from becoming overly elongated and narrow. The tree allows queries for the r nearest neighbors of any given point, with the option to return only those within a certain maximum distance. Furthermore, the r approximate nearest neighbors can be queried with a significant increase in efficiency.

It can be used to calculate the shortest distance between nodes in a grid network by examining two sets of decimal degrees. However, for large dimensions like 20 or more, do not anticipate this algorithm to perform much faster than a brute-force approach. High-dimensional nearest-neighbor queries remain a considerable open challenge in the field of computer science. It is utilized in this thesis to calculate the shortest distance between buses and new charging stations in the power grid to install new infrastructure to the bus that is within the shortest distance.

4

Methodology

The methodology section concerns solving the musk-model for a real-world data set of Northern Norway, adapting certain terms in the mathematical model, and implementing new constraints and expressions in the model's objective function. When solved, the optimal locations to install new charging stations are input for the PyPSA model. They act as a load in the power system, drawing active and reactive power from it. This model installs the charging stations for BETs to the grid and then optimizes the grid. Resulting in an interesting framework for analyzing the impacts of new charging stations on the Norwegian power system.

4.1 Musk-model for a case study in Norway

4.1.1 Data gathering

This section will explain how the data is gathered. Primarily the data sets come from secondary sources. To solve the musk-model for a case study in Norway, data is gathered from *Geodata AS*. They act as the Norwegian distributor for ESRI software. They have a deal with several academic institutions in Norway. As a result, students from the university in Tromsø (UiT) can apply to use the data set for free. Geodata offers many interesting data sets for GIS software, including maps with land-use classification, properties, demography, traffic, avalanches, and more. For this thesis, access was granted to use the traffic map containing parking, airports, resting lots along roads, toll booths, charging stations, charging points, traffic flow, and more. The data in this map belongs to several different firms. Some from the company itself, *Geodata AS*, other contributors are *the Norwegian mapping authority*, *the Norwegian Public Roads Administration*, *Entur AS*, and *webcams.travel*. The features from the traffic data set are mainly based on *the Norwegian Public Roads Administration* and *Entur AS*, making the sources primary. Other parameters for the case study are based on secondary sources and assumptions.

The software used for managing maps and data sets is ArcGIS Pro, distributed by ESRI. It is available for free under an academic license for certain institutions. Another option is to use QGIS, which is free and open-source. The traffic data set is added to ArcGIS PRO as an ArcGIS database for which the features are implemented to the map. The features of interest can be visualized in figure 4.1 to 4.2. Some computational issues are encountered when including the full data set for the whole country for the musk-model (MILP). Therefore, a cutout is selected in the region North of Steinkjer. This issue will be explained further in the next section.

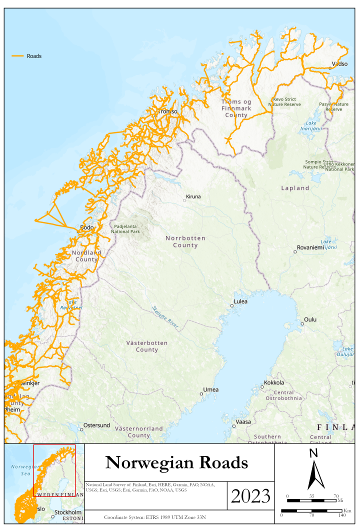

Figure 4.1: Road Network.

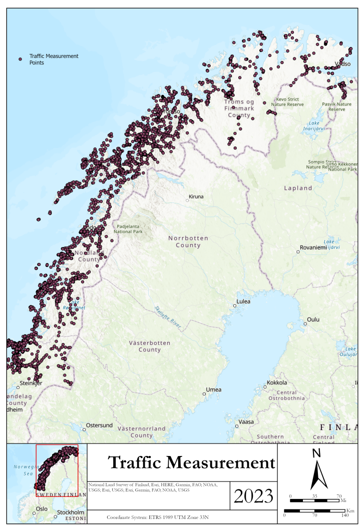

Figure 4.2: Traffic Measurement.

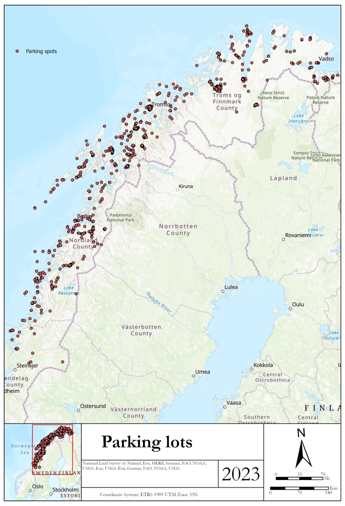

Figure 4.3: Parking Locations.

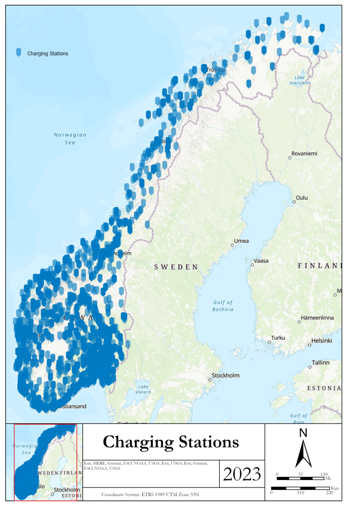

Figure 4.4: Charging Stations.

The figures represent critical data for the Musk-model, as it relies heavily on geographical information. The road network in figure 4.1 includes traffic measurement points extracted to a new map in figure 4.2. This data is needed to calculate each grid cell's average daily traffic flow. Parking locations in figure 4.3 are considered suitable locations for establishing new chargers, and charging stations in figure 4.4, are needed to know where the demand is already met. The *Grid Index Feature* tool in ArcGIS Pro is used to make a grid where each grid cell i is a square with a length of 5km along the existing infrastructure, such as charging stations, parking lots, and roads.

Figure 4.5 shows a full grid network covering the whole region. For the musk-model, this creates issues concerning the data set being too large, as discussed in the theory section concerning problematic features of MILP models. Instead, the grid network is implemented only along locations of interest (roads, parking lots, and charging stations), as seen in figure 4.6. There will be no charging demand in certain locations, such as mountains, forests, etc. This causes the model to iterate through significantly fewer instances when solving. The resulting model is, therefore, computationally tractable. A more computationally tractable implementation of the grid cells can be seen in figure 4.7.

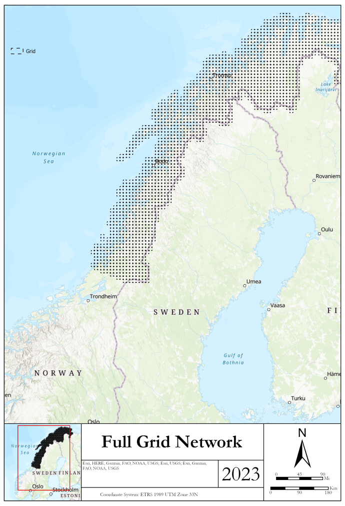

Figure 4.5: Full Grid Network.

Figure 4.6: Aggregated Grid.

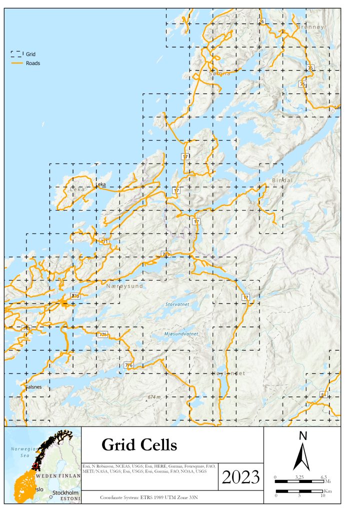

Figure 4.7: Grid Cells.

4.1.2 Traffic flow in grid

First, the centroid coordinates (in decimal degrees) for x and y are calculated and assigned to each cell using the *Calculate Geometry Attributes* data management tool [59]. This cannot be done after the next step. The traffic flow for each grid cell can be calculated in Argis Pro using the analysis tool *Spartial Join* [60] on the grid and the traffic points. The traffic points in each cell are then averaged for every cell in the grid. For grids with information missing, the tool

Fill Missing Values (Space Time Pattern Mining) is utilized to insert averaged values of surrounding grid cells [61], see figure 4.8.

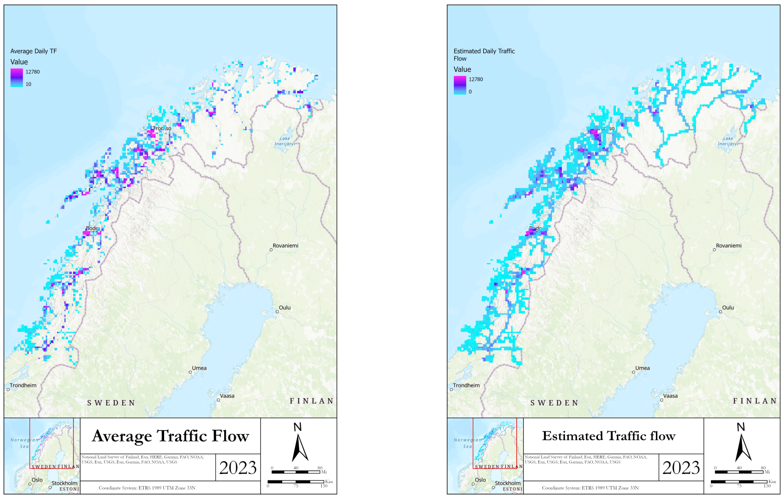

(a) Averaged TF from measurement points.

(b) Estimation of missing values.

Figure 4.8: Averaged daily Trafic Flow (TF) in 2022.

4.1.3 Land-use classification

The only data set missing for the case study is the land-use classification, multiple land-cover classifications are available, but the land-cover only describes whether the land is classified as woods, mountains, etc. Places of interest are residential and commercial areas where people stop to rest. Online searches were unsuccessful, except for a data set from Geonorge (driven by the Norwegian Mapping Authority). No further attempts were made to achieve this after not getting access to the national land-use map from Geonorge. It could be created with machine learning models, but that is out of the scope of this thesis. Instead, each area is regarded as equally suitable for installing charging stations. Then it follows that $A_i = A$, where A is the total area of a cell in meters. Since the length of each grid cell is 5km, the total area is 25km per grid cell. This reduces Eq ((3.15)) to $v_0 = v_i$.

4.1.4 Capacity, battery capacity and charging time

The upper bound or total number of chargers per station n_j is selected to be four as the governmental policy recommends fewer chargers per station to spread the total number of charging stations over a bigger area to enhance the availability of charging [62].

Scania and Volvo have developed functional BETs and probably represent the biggest market share of BETs in Norway. A reference vehicle is selected to represent the average battery capacity α. Little exists in literature or official reports. Figure 4.9 shows a snapshot from Scania's website where α is set to the usable battery capacity of 468 kWh. The installed capacity is 624 kWh, but because of the State of Health (SoH), only 468 kWh are usable (75% of full battery).

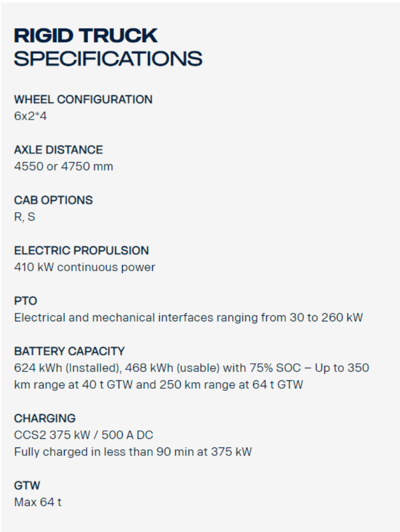
RIGID TRUCK SPECIFICATIONS

WHEEL CONFIGURATION
6x2*4

AXLE DISTANCE
4550 or 4750 mm

CAB OPTIONS
R, S

ELECTRIC PROPULSION
410 kW continuous power

PTO
Electrical and mechanical interfaces ranging from 30 to 260 kW

BATTERY CAPACITY
624 kWh (Installed), 468 kWh (usable) with 75% SOC – Up to 350 km range at 40 t GTW and 250 km range at 64 t GTW

CHARGING
CCS2 375 kW / 500 A DC
Fully charged in less than 90 min at 375 kW

GTW
Max 64 t

Figure 4.9: Scania, rigid truck specifications. Retrieved from [63].

Since the usable battery capacity is 468 kWh with a charging time of 90 minutes, the maximum power for which the battery can charge is at least 312 kW since it is the average charging power. The charging time t can be calculated based on usable battery capacity and the charger's power. From Table 1 in [64], the power limit for the planned chargers is 250 kW which is below 312 kW, resulting in a slower charging time for this type of charger. Therefore, t can be calculated by dividing the usable battery capacity by the power limit of the charger. Resulting in a charging time t of 1.872 hours or 112 minutes. It is important to note that if two vehicles charge at the same charger (parallel circuit), the voltage will be constant, but the current and power will be split between the two vehicles by Kirchoff's current and voltage law. And thereby, the charging time will increase.

4.1.5 Adaption rate and charging possibility

The adaption rate u can be derived from [65] assuming that private cars, vans, trucks, and buses are the main contributors to the traffic measurement points. Then v_0 is the number of BETs (455) divided by the total of the main contributors (3 497 790). Resulting in $v_0 = 0{,}013\%$. However, this adaption rate is too low for the model to be profitable. Instead, the new chargers will be available for every EV to finance the stations until a substantial amount of BETs are utilized. This is possible since EVs and BEVs use the same connector for charging, usually CCS2. In this instance, the adaption rate v_0 is 17.8%. But still, the charging time and battery capacity will be dimensioned for BETs to ensure that the capacity at the station is maintained if the number of BETs increases. The charging possibility can be viewed as the time spent charging during 24 hours. Public chargers are assumed to be used once daily to charge the battery fully. Each charger can be used a maximum of seven times daily ($m \approx 7$), based on charging time t from 08:00 to 20:00 (12 hours). During the night, the BETs charge at a private charger owned by the company of the BET or is stationary and not charging. The charging possibility is then $u = t/24 = 7.8\%$.

4.1.6 Costs

Reviewing relevant literature is necessary to determine the costs used in the case study. Since most costs in literature are in USD or EUR, a fixed value is determined throughout the thesis for converting the currencies to NOK since currencies fluctuate. See Eq (4.1) and Eq (4.1.6).

$$1\ USD = 10,5 NOK \tag{4.1}$$

$$1\ EUR = 11,5 NOK \tag{4.2}$$

Another value that is hard to determine a fixed value for is p_e, the average price of electricity in (NOK/kWh). This value is derived from *Statistics Norway* (SSB), taking the average of the mean value for every quarter during 2020, 2021, and 2022, resulting in $p_e = 1.11$ NOK per kWh [66]. The prices are for households and include grid rent and taxes. It can be visualized in figure 4.10. An average value is calculated based on the record low prices during 2020 and record high prices during 2021 and 2022. The price might be somewhat lower in the Northern part of Norway, but it is projected that the price will rise in this region due to Northern Norway mowing towards a deficit of electricity.

A new parameter c_j^{inv} is introduced to represent the total investment cost re-

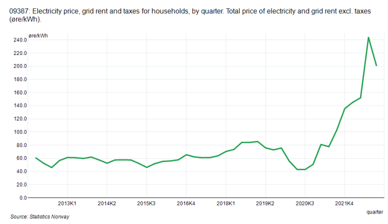

(a) 2013-2022

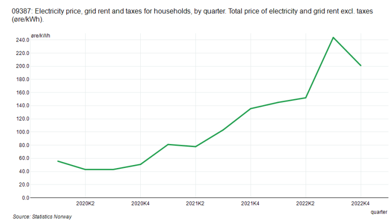

(b) 2020-2022

Figure 4.10: Electricity price in Norway. Retrieved from [66].

lated to installing a charger, including operational expenses, material costs, grid reinforcement costs, transformer costs, capital expenditure, and maintenance and repair costs. The value of c_j^{inv} is based on *Table* 1 in [64], which describes the cost of installing a "Super-fast DC public charger" hereby denoted as a rapid charger. The total investment cost for one rapid charger is 125 000€ = 1 437 500 NOK, with a ten-year station lifetime. The investment cost must be aggregated into daily costs, resulting in c_j^{inv} = 3938 NOK. As a result, the cost per station j can be written:

$$c_j = (\cdot c_j^{inv} + c_j^r) \cdot n_j + p_e \cdot \alpha \cdot q_j, \tag{4.3}$$

Two new parameters are introduced to represent governmental incentives in the model. They are based on the total amount of incentives In_t delegated to building new rapid chargers in areas with insufficient amounts and the amount delegated for investing in a new charger at a site In_j, giving a reduction to the investment cost c_j^{inv}. The total cost for each charging station is then:

$$c_j = (\cdot c_j^{inv} - In_j + c_j^r) \cdot n_j + p_e \cdot \alpha \cdot q_j, \tag{4.4}$$

In 2022, the Norwegian government delegated 100 million NOK to ENOVA [67]. They are responsible for investing the incentives to charging station builders, with an upper bound of a given percentage of the investment cost. For this thesis, an upper bound of 80% is selected. This means ENOVA can maximally delegate 80% of the investment cost for installing a new charger. Additionally, In_t must be transformed into daily costs by dividing 100 million NOK by 365.

The parking fee c_j^r is determined by the number of parking slots occupied by the installed chargers. It is assumed that each charger has two outlets. Thereby, one charger occupies two parking slots. It is assumed that the parking lot owners have agreed on a fixed amount of 200 NOK/day for each slot occupied. This results in c_j^r = 400 NOK/day for each charger installed at a site. Further development of new constraints regarding the parameters is explained later.

4.1.7 Profit

Determining p, the cost of charging per minute, is tricky. These prices fluctuate, and there is little literature regarding this topic as the station owners decide the price. There is also a different price related to regions (mainly North and South Norway) in Norway. Since the electricity price was determined for both South and North, the same will be utilized for p. A snapshot of 2023 for the price for both regions will be averaged. The price for fast charging will be based on prices from *Mer Norway AS*, which *Statkraft* (State driven power company) operates. Respectively the prices for South and North are 6,99 and 8,39 NOK/kWh, assuming the user is a registered customer. Therefore the value of p is 7.69 NOK/kWh.

4.1.8 Model improvements and new features

A few adaptions are made to implement a case study in Norway based on the previously described musk-model. The original model forces a number of new charging stations N (eq. (3.7)) to be built by selecting an integer as a parameter. This causes the model to build new stations even when the objective function is negative, meaning negative profits. To develop the model further, the main objective is to get the model to decide an optimal number of new charging stations N to be built while ensuring that the objective function is not negative. The optimal number of N can be achieved, simply by making it a decision variable, instead of a parameter, as seen in Eq (4.6). However, given the current constraints and the parameters used in this case study, the profit would be negative if any number of new charging stations were installed since the cost of building one station is much higher than the profit per station. This results in zero new stations and an objective function of zero.

Therefore it is necessary to implement a new constraint to the mathematical model. Based on the total amount of incentive that ENOVA receives from the government to use on charging infrastructure found in ENOVA's annual report for 2022 [67]. The amount of NOK 100 million is selected for the total incentive for building new fast charging stations, In_t. While In_j is, 80% of the investment cost c_j^{inv}. A new constraint is implemented to ensure that the sum of incentive per charger n_j does not exceed the limit of 100 million NOK, as seen in Eq (4.14).

$$\sum_{j=1}^{J} In_j \cdot n_j = In_t \tag{4.5}$$

Based on the thoughts outlined above, the full mathematical model introduced in the section [add section] has been modified and, as a result, can be expressed in eight equations, Eq (4.6)-(4.14):

$$MaximizeProfits\left(x_j, n_j, q_j, N\right) = \sum_{\text{j=1}}^{\text{J}} \left[p_j \cdot t_j \cdot q_j - c_j\right], \quad j = 1, 2, \ldots, J \tag{4.6}$$

Subject to,

$$c_j = (c_j^{inv} - In_j + c_j^r) \cdot n_j + p_e \cdot \alpha \cdot q_j, \tag{4.7}$$

$$q_j \leq n_j \cdot m_j \tag{4.8}$$

$$q_j \leq \sum_{i=1}^{I} r_{ij} \cdot dr_i \tag{4.9}$$

$$\sum_{j=1}^{J} x_j \cdot r_{ij} \leq 1 \tag{4.10}$$

$$n_j \geq x_j \tag{4.11}$$

$$n_j \leq l_j \cdot x_j \tag{4.12}$$

$$\sum_{j=1}^{J} x_j = N \tag{4.13}$$

$$\sum_{j=1}^{J} In_j \cdot n_j \leq In_t \tag{4.14}$$

$x_j, n_j \leq 0$, where x_j and n_j are integers,

where $j = 1, 2, \ldots, J$ and $i = 1, 2, \ldots, I$.

This model will select optimal locations for areas to install new charging stations based on where it is most profitable. Existing chargers are considered by diminishing demand from cells where they are present. Finally, optimal locations and the yearly profit/costs of installing these new chargers are revealed. If there are profits, it can be used to determine whether the project is profitable during the station's lifetime by discounting cash flows and determining the net present value. The locations can be extracted as shapefiles for GIS or as a data frame for further analysis.

4.2 Model of the Norwegian grid

The output from the musk-model will be soft-linked with PyPSA-eur for further analysis. First, a base network for Norway is established using PyPSA-eur, figure 4.11. The reference year 2013 is selected due to computational difficulties creating new cutouts from ERA5 and Sarah. 2013 is also the standard year included with PyPSA-eur since it is regarded as a normal year for the climate (rain, wind, solar irradiance, etc.). This is important when calculating the potential for renewables. The base network consists of 380 kV voltage lines. After the base

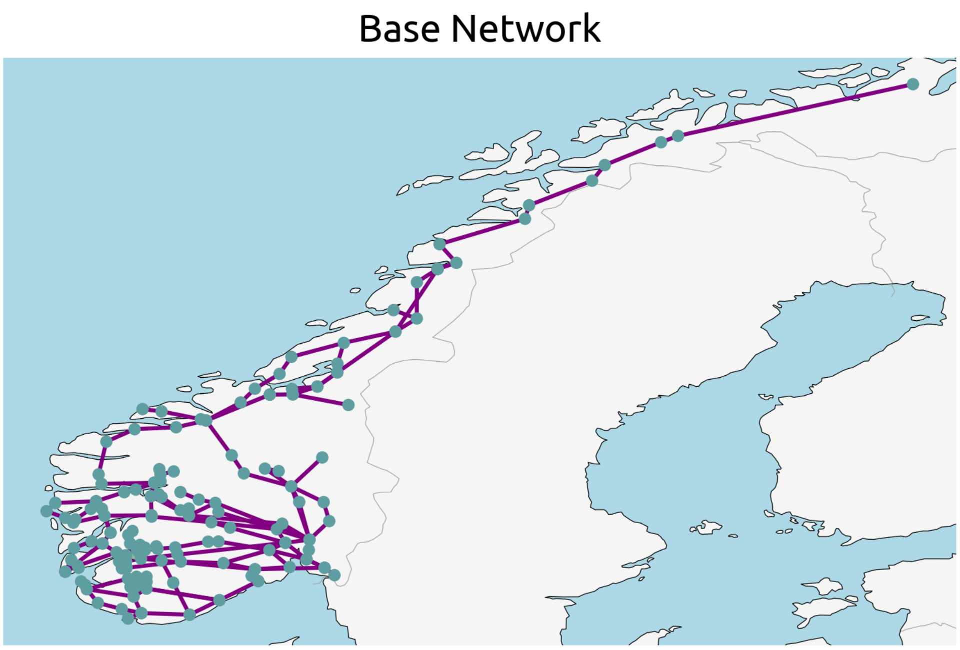

Figure 4.11: Base network of Norway.

network is established, PyPSA-eur is instructed to add underlying electricity to the grid network. The network is manually configured in Python to implement new buses, lines, links, and loads representing the new charging stations connected to the grid. The charging station locations for the whole of Norway, including existing and new stations from the musk-model, are saved into a csv file and read into PyPSA as a pandas DataFrame, which includes charger capacity, latitude, and longitude position. The general idea is to use network components from PyPSA to implement the existing 26 541 chargers and the 35 new ones to analyze impacts of new loads with 250 kW drawing active power from the power system. The electrical network already includes generators and buses. A function is implemented to calculate the shortest distance between chargers and network nodes to connect links to the corresponding buses, for which a *binary k-d tree algorithm* is used. Every charging station node iterates

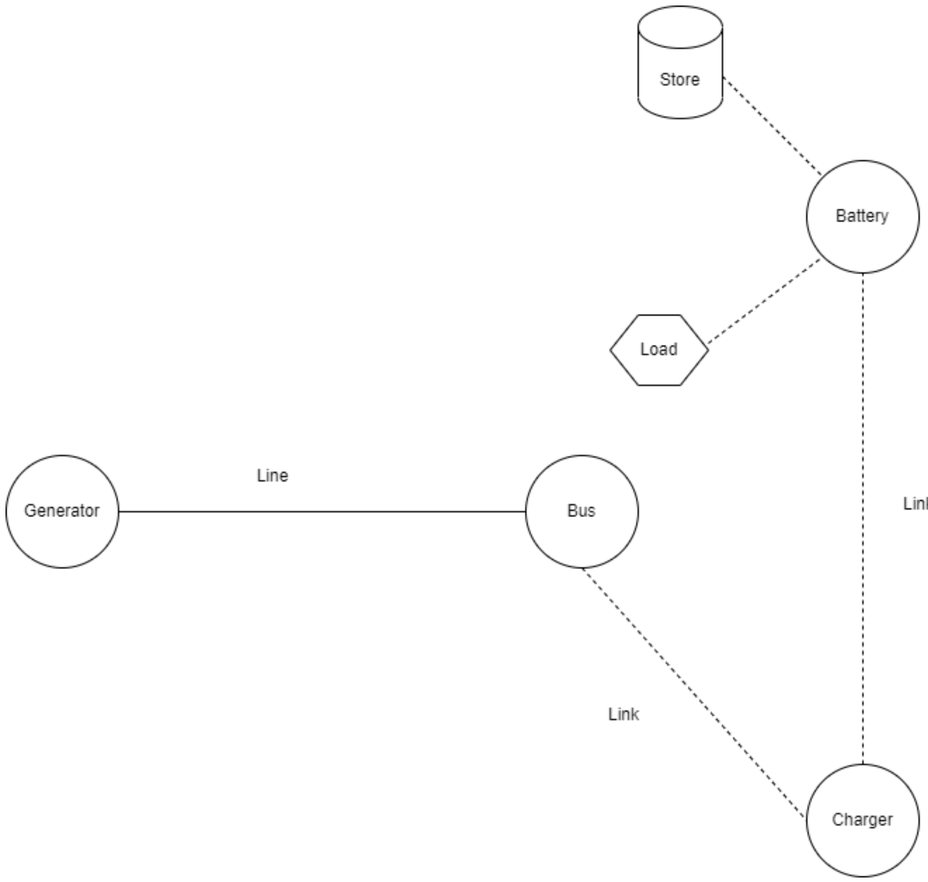

Figure 4.12: Architecture for implementing chargers.

through all the buses in the network to find the closest connection point. Then the charger is linked to a battery (468 kW) with a *load* and a *store* component. The architecture can be seen in figure 4.12. An artificial time series for 2013 represents EV usage to simulate load in the battery. See figure 4.13.

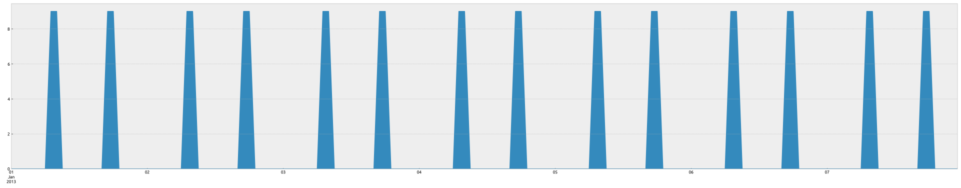

Figure 4.13: Weekly EV usage.

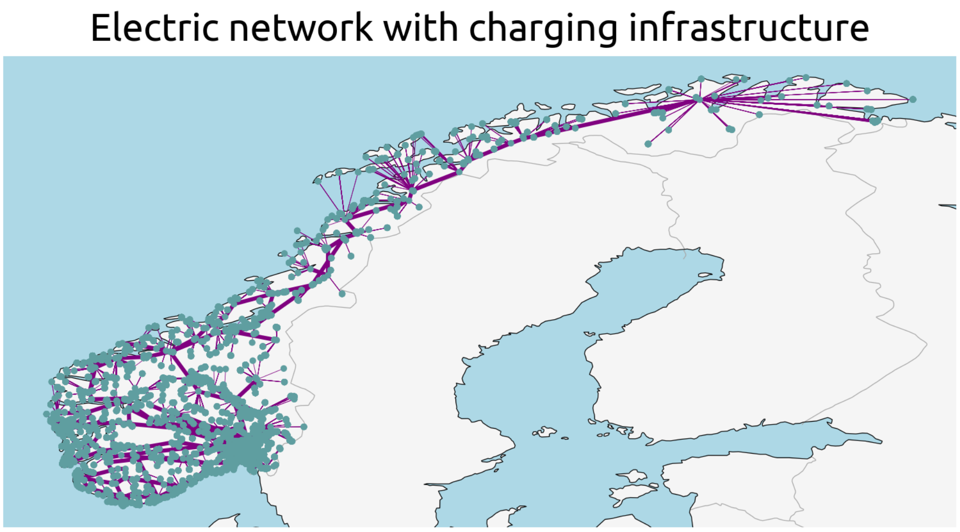

Figure 4.14: Charging stations connected to the grid.

The new electric network is then saved manually, replacing the original. Figure 4.14 shows the full electrical network with chargers.

A network with this amount of nodes requires solid computational power. The network is clustered into 66 nodes using a *k-means* based clustering technique to make the power system model more computationally tractable. Finally, the network is solved by optimizing the linear power flow, and the time resolution is averaged over daily (24-hour) snapshots, as seen in figure 4.15. A network without containing any chargers is solved for comparison using the same amount of clusters and configuration.

Clustered into 60 nodes

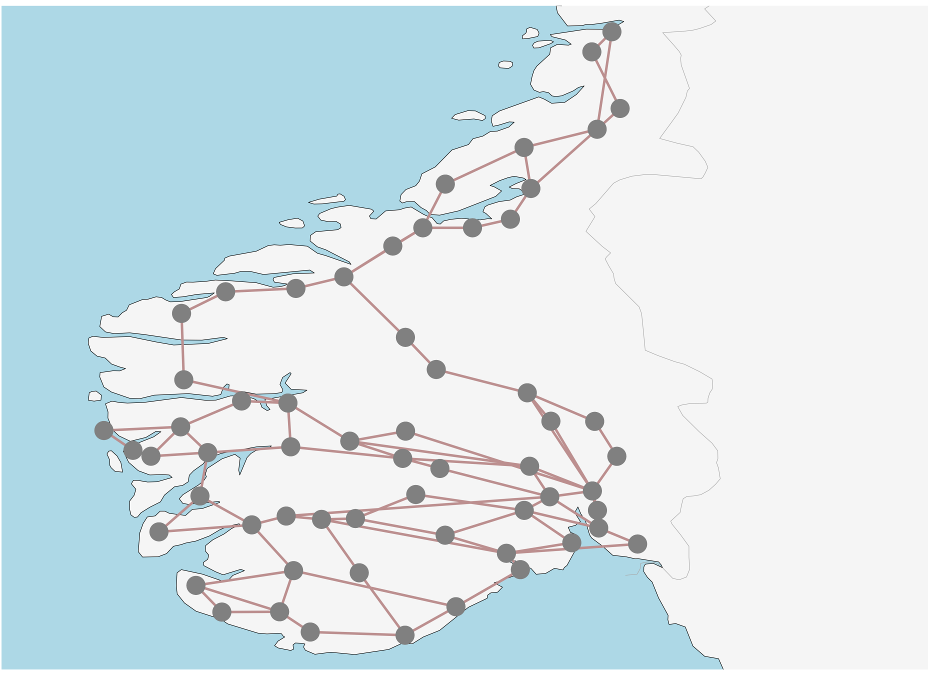

Figure 4.15: Aggregated nodes.

5 Results

This section shows the results of the optimal rapid charger locations followed by a sensitivity analysis on daily charging m, average battery capacity α, incentive per charger In_j, the price for charging at rapid charger P, and charging time t. The allocation of the new and existing rapid chargers will then be analyzed in the Norwegian grid network. Analyzing load distribution, prices, line loading, line expansion, and optimal power capacity. To reproduce the same results, visit the GitHub repository *github.com/o2i/Masters-Thesis*, [7].

5.1 Optimal location

The result of the optimal allocation of 15 new charging stations is displayed in figure 5.1. In total, 35 new rapid chargers are installed at these stations. The ones with the highest capacity are located in Harstad, along the highway (E6) in between Narvik and Bardu, Finnsnes, Tromsø, and two stations in Alta. The only station with a capacity of 3 chargers is located outside Karasjok, at Riksvei 92. This road is a link between Karasjok and Finland. No stations have a capacity of two chargers. There are eight stations with a capacity of one charger. Five are located in Nordland County, while the remaining three stations are located north in Finmark County. The ones in Nordland are located in Forvik, two at Austbø, Riksvei 812 between Rognan and Grønli, and outside Bodø at Nordvik. The remaining stations in Finmark are located outside Lakselv, Honningsvåg, and at Riksvei 98 between Lebesby and Børselv.

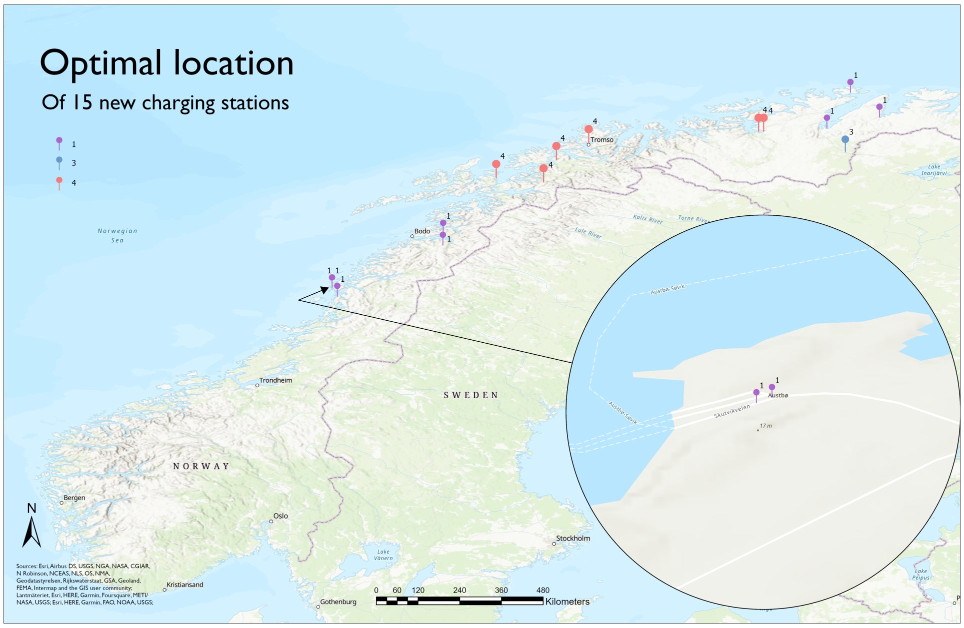

Figure 5.1: Optimal location of 15 new charging stations, with a total of 35 rapid chargers.

Overall, the stations are widely scattered over the area of interest, except for Alta and Austbø, where two sets of stations are close. Since the model selects two charging stations for Alta and Austbø, it indicates that the current demand for EV charging is not yet met, which means that the charging demand is much higher than what the currently existing chargers can supply, and therefore a profitable location for installing a new charger.

In general, the selected locations seem valid concerning where it would be logical to install a station. All are located at parking lots near cities, villages, and roads or highways with high traffic flow. The new stations can reduce driving range anxiety for both EVs and BETs, while the builder can operate with a profit during the station's lifetime.

5.1.1 Sensitivity

To understand how different parameters affect the objective function of the model, sensitivity analysis is utilized on charging times per day for charger (m_j), battery capacity (α), the upper bound of chargers in each station (l_j), EV adaption rate v_0, price of charging at rapid charger (p), charging time (t), the incentive per charger (In_j), and adaption rate v_0. The analysis is based on the parameters used to find the optimal location of 15 new rapid charging sites, visualized in figure 5.2. The interval from zero to seven is selected since

m can have a maximum of seven vehicles charging from 0-100 % during a day. The only sensible values for m are in the domain of [0,7]. To display multiple functions in the same graph, it is easiest to accomplish using the same domain in the x-axis. So, for instance, l_j, is tested for values in the range [0,14] chargers. To adjust the function within the same domain as m, it is multiplied with a factor for each time step in the graph. The optimization is iterated using a for loop, changing values for $l_j = i/7 \cdot k$, where $i = [0, 7]$ and $k = 2$. Resulting in the actual domain of D_{l_j} = [0,2,4...,14]. The same is done for the remaining parameters but with a different k to reflect sensible values for each parameter. Such that, battery capacity α ranges from 56-450 kWh, l_j ranges from 0-14 chargers, EV adaption rate v_0 ranges from 0-100%, p ranges from 1.1-15.1 NOK, t ranges from 30-114 minutes, incentive per charger In_j ranges from 0-100 %.

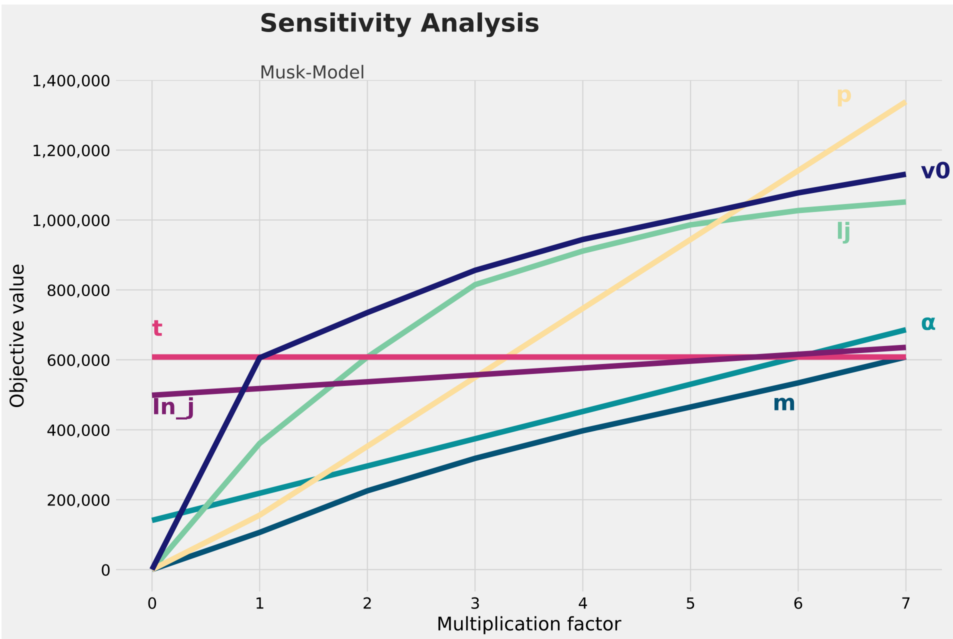

Figure 5.2: Sensitivity analysis on m, α, l_j, p, t, In_j, v_0.

During the time steps, p, l_j, and v_0 are the biggest contributors to maximizing profit (objective value). The charging price at a rapid charger p is linearly related to the objective value, while l_j and v_0 have a damped exponential growth. They both have an impact on the demand (where the maximum value of the demand is the full traffic flow). l_j and v_0 have a direct impact on the final demand as they are limiting traffic flow but stagnate when the maximum amount of traffic flow is represented as the demand. The objective value quickly rises before the upper bound of demand is met. When the demand is met, the growth stagnates. The charging time t does not impact the objective function since it cancels out when multiplied by both p and p_e. The battery capacity α

and incentive per charger In_j are linear. The number of daily charging times per day m is approximately linear concerning maximizing profits and contributes slightly less than α and In_j.

The mathematical model for the musk-model is set to maximize the daily profits for implementing the new stations. In the optimal case from 5.1, the daily profits from installing the new charging sites is 608 092 NOK. Resulting in a yearly profit of 222 million NOK, which is not a realistic case and will be discussed further in the next chapter.

5.2 Impacts of new loads on the grid

These results are obtained from soft-linking the optimal locations from the musk-model with PyPSA-eur by adding the total amounts of chargers in Norway to the system as loads that draw 250 kW of active power from the system. Comparing a case without and with the new installation. These networks contain the overlying topology of the Norwegian grid, including generators, clustered buses, storage units, links, stores, carriers, transformer types, loads, lines, and line types. This is an electricity-only study, meaning demand from all other sectors is excluded.

The distribution of loads is compared in figure 5.3. The installed amount of chargers is 26 599, which especially affects the grid in buses near highly populated areas because population and installed chargers correlate. The total capacity for all the chargers is 1.39 GW. All the chargers are utilized to charge from the same repeating time series, representing an artificial usage pattern for EVs. The distribution of loads is largest in the region around Oslo. The bus furthest north represents the total load that Northern Norway has on the grid. The load distribution without chargers represents loads created by consumers and establishments, which during the year added a load of 5.3 TW to the grid. The total change in active power consumption between the two cases is 14 541 GW. The grid, in total, had an increased load of 14.5 TW during the year due to the new chargers.

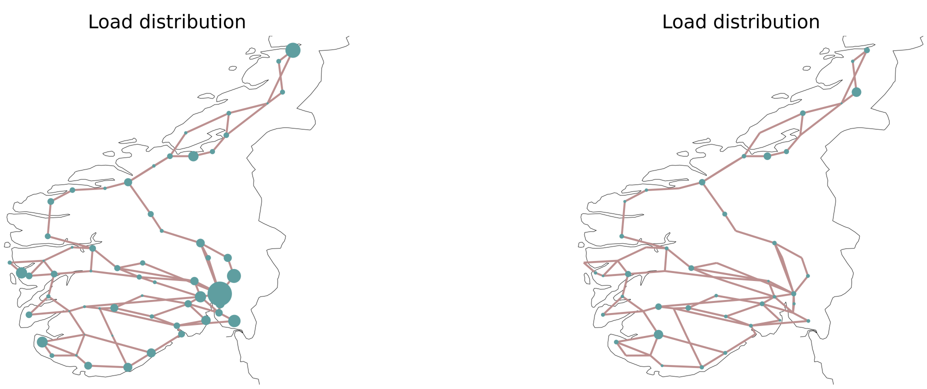

(a) With chargers. **(b)** Without chargers.

Figure 5.3: Comparison of load distribution.

A line expansion is necessary to address the new demand from increased loads. The comparison of line expansion can be seen in the horizontal bar plot in figure 5.4. To meet the new demand, the new lines are expanded to handle an additional apparent power flow of 471 GW.

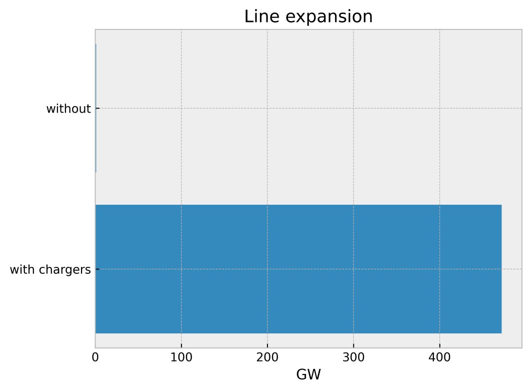

Figure 5.4: Comparison of line expansions.

The load distribution during the year is displayed in figure 5.5. Where the highest loads are during the winter months. The load distribution pattern during the year is the same for both cases since additional load from the chargers is aggregated into 24-hour snapshots and is represented by a cyclic time series, only increasing the magnitude of load distribution. For further analysis of line loading and electricity prices, the 21st of January and July 30th are selected to represent a case with high and low demand.

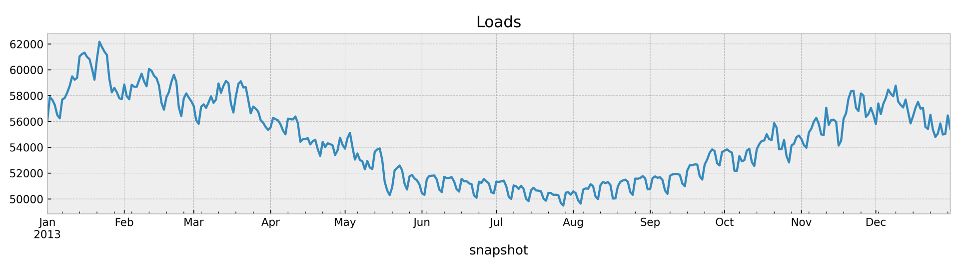

Figure 5.5: Load distribution during 2013.

Figure 5.6 displays how the chargers are loading the lines during the 21st of January. This is a date when the load from consumers is high. The load is probably high since it is during the coldest months in Norway, and the heating of homes is causing a higher load on the grid. The highest loaded lines are in Trønderlag. In comparison, figure 5.6b displays how lines are loaded only considering loads from consumers and establishments. It is important to note that the lines are expanded to handle larger loads in figure 5.6a.

Figure 5.7 displays how the chargers load the lines on the 30th of July. This is a date when the load from consumers is low. The load is lower due to the warmer weather, and less heat is required to warm up households. The highest

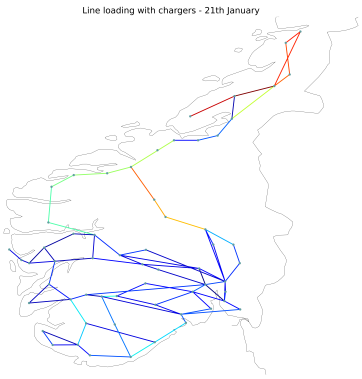

(a) With chargers.

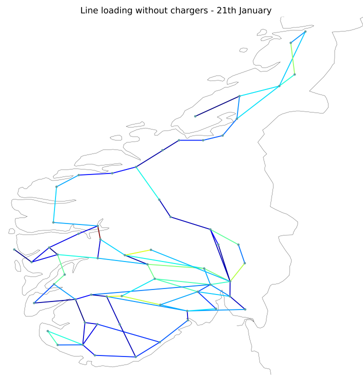

(b) Without chargers.

Figure 5.6: Line loading 21st of January.

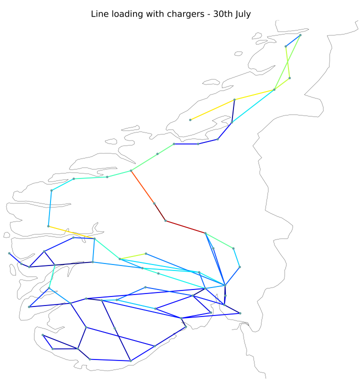

(a) With chargers.

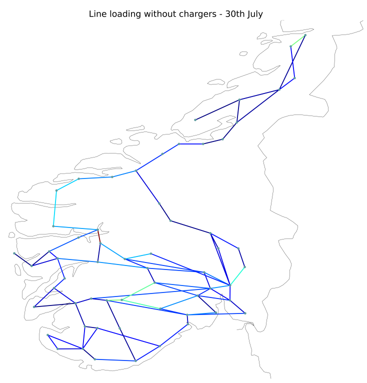

(b) Without chargers.

Figure 5.7: Line loading 30th of July.

loaded line is located between Orkanger and Rindal. It is a 380 kV line with a newly installed maximum capacity of 6314 MVA. Without chargers, the maximum capacity is 0,2 MVA. The cost for installing this line can be calculated by multiplying the capital cost (for increasing the limit of apparent power flow by 1 MW) by the maximum capacity of the case with and without chargers. Resulting in a capital cost of 138.4 million NOK for expanding the line.

Figure 5.8-5.9 displays the marginal price for which electricity production is profitable during the 21st of January and the 30th of July. The average price in Norway for installing all the chargers is 1.05 NOK/kWh, while without chargers, it is 0.38 NOK/kWh. After installing the chargers, the marginal price must be raised by 279 percent to ensure profitability at the given date. The average marginal price with chargers on July 30th is 0.57 NOK/kWh, while without chargers, it is 0.38 NOK/kWh, meaning an increase in the marginal price of 150 percent on July 30th. The cheapest locational prices are in Northern Norway,

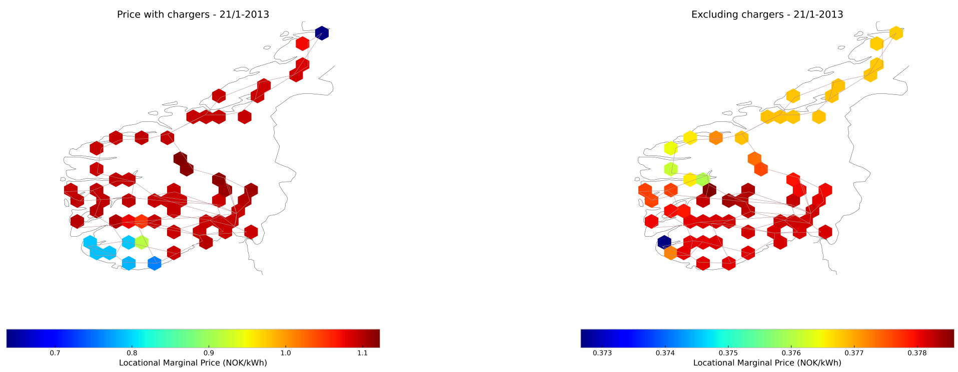

(a) With chargers. **(b)** Without chargers.

Figure 5.8: Prices for 21th of January.

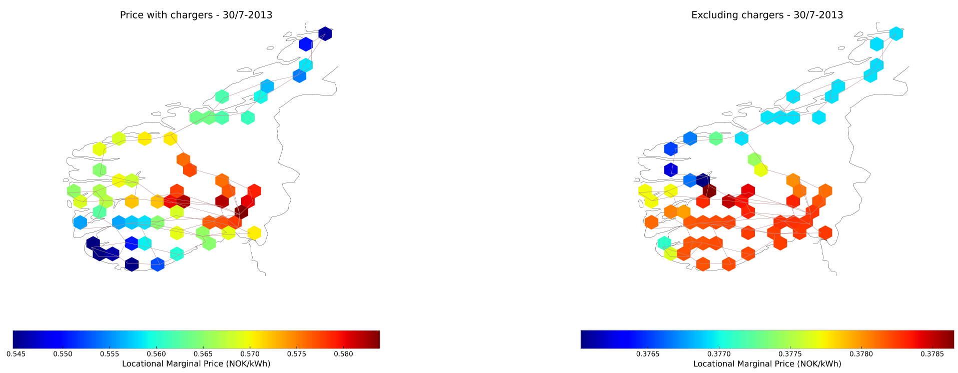

(a) With chargers. **(b)** Without chargers.

Figure 5.9: Prices for 30th of July.

Agder, and Rogaland after installing chargers, while the cheapest locational prices are in Northern Norway, Trøderlag, Vestlandet, and Stavanger, without installing chargers.

The optimal expansion of increasing nominal power and capacity for generators and storage units can be seen in figure 5.10. The largest capacity is onshore wind and solar generation, with 142 GW and 90 GW in nominal power. The third largest expansion is in hydro, with a nominal power of 29 GW. Pumped hydro storage, offshore wind, run of river, and CCGT have a combined nominal power capacity of 6 GW. Solar and onshore wind nominal power capacity is expanded with 90 and 138 GW. Meaning that a huge expansion of new wind and solar parks is necessary.

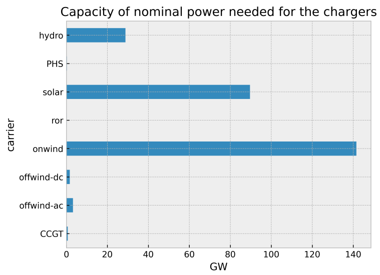

(a) Max capacity.

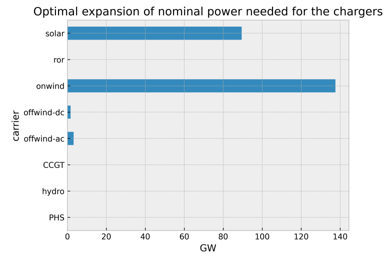

(b) Expansion.

Figure 5.10: Capacity and expansion of generators and storage units.

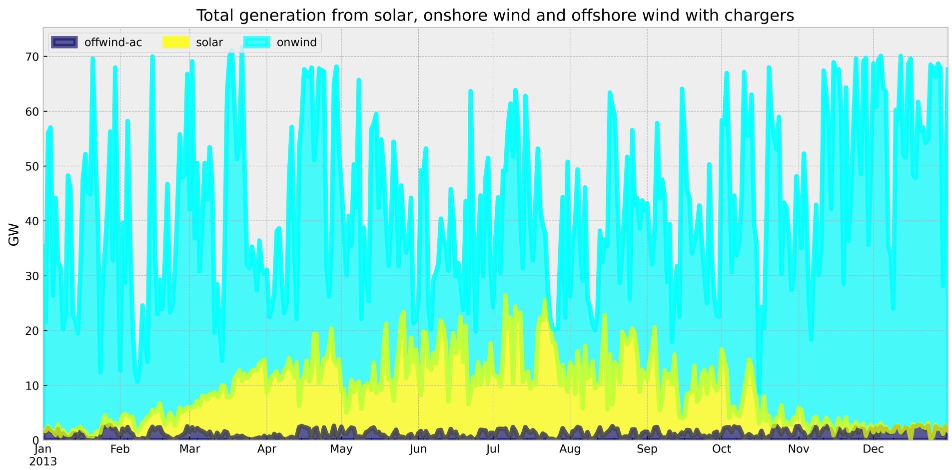

Figure 5.11: Generators above 1.7 GW with chargers.

The time series of onshore wind, solar, and offshore AC wind is displayed in figure 5.11. It displays electricity production above 1.7 GW from generators in the case with installed chargers. Energy production from these carriers is highly fluctuating based on the weather. Solar generation is highest in the summer since solar irradiation is highest in these months. It fluctuates between a maximum of 24 GW and a minimum of 0 GW. Wind generation fluctuates between a maximum of 69.4 GW and a minimum of 1.29 GW.

In the case of excluding the installation of chargers, the time series for electricity production from generators bigger than 1.7 GW are displayed in figure 5.12 with a maximum onshore wind production of 4.4 GW and a minimum production of 0.05 GW. Compared with figure 5.11, installing chargers needs an electricity production that is 65 GW higher from onshore wind.

However, the largest contribution to producing electricity in Norway is from hydropower. The total state of charge from hydropower and PHS is displayed

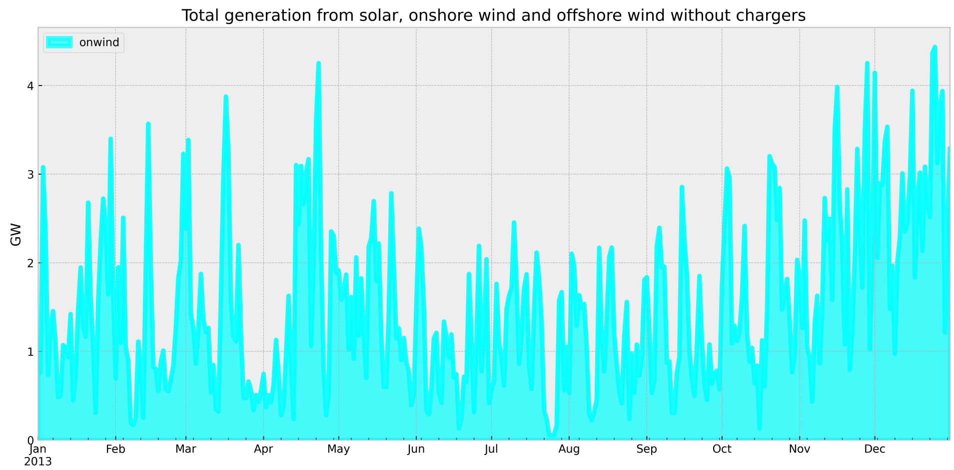

Figure 5.12: Generators above 1,7 GW without chargers.

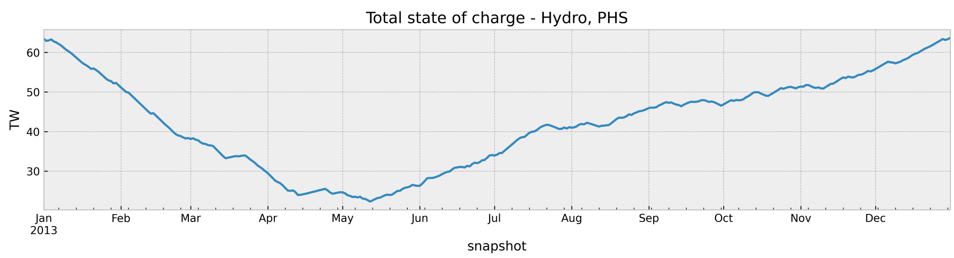

Figure 5.13: State of charge, hydro, and PHS.

in figure 5.13 with chargers installed and shows how the total capacity varied during the year. In the beginning, the magazines have a capacity of over 60 TW. While being slowly depleted until mid-May, before filling up once again during the rest of the year. Figure 5.14 displays the distribution of electricity production from hydro, onshore wind, solar, CCGT, offshore wind AC, offshore wind DC and PHS. Hydro accounts for 99.19 percent of the electricity production, while the remaining accounts for 0.81 percent of the total electricity production.

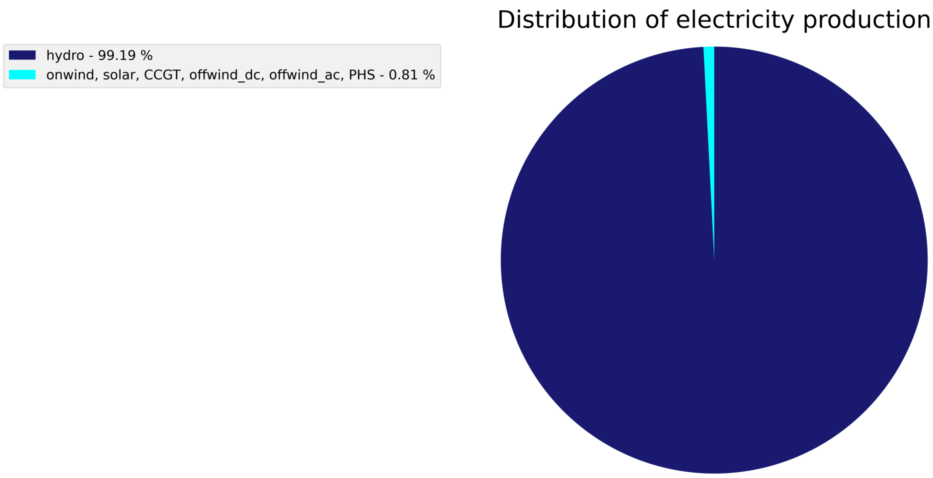

Figure 5.14: Distribution of electricity production by carriers.

The PyPSA-eur mathematical model is designed to minimize the total system cost. The analyzed networks are considering the cheapest expansion and building of lines, generators, and storage units, which satisfies the new electricity demand. The annualized total system cost for implementing the chargers to the Norwegian grid is 280 billion NOK, while the case excluding chargers has an annualized total system cost of 2.34 billion NOK. The suggested implementation of chargers to the grid will increase the annualized total system cost by approximately 1200 percent.

6

Discussion

The high daily profits from the musk-model demonstrate how profitable charging stations can be in the future, and the optimal allocation of charging stations provides the planner with a solid base for selecting the most suitable locations for implementing new chargers based on where demand from other charging sites is not yet met. The sensitivity of charging times per day for charger (m_j), battery capacity (α), the upper bound of chargers in each station (l_j), EV adaption rate v_0, price of charging at rapid charger (p), charging time (t) and the incentive per charger (In_j) gives insight on how the different parameters affect the objective value of the musk-model.

The soft-linking with PyPSA-eur gives the planner a solid open-source framework for investigating how the installations affect the national power grid. It is possible to investigate how the new loads will affect components in the power grid, allowing the planner to analyze lines, generators, storage units, buses, links, and loads. This is important for the planner since new installations in the grid can raise marginal prices, as demonstrated. The grid operators raise electricity prices to compensate for higher marginal prices, leading to higher costs for station owners, which again must compensate by raising the price for charging, which can reduce the EV penetration rate, affecting the objective value in the location-allocation model, resulting in having to reassess the model.

The soft-linking between the models provides an open-source framework for students, researchers, and planners to investigate the potential capacity of upgraded or newly installed generators and the total electricity produced from renewable sources. This shows where new generators can be placed to satisfy increasing demand from charging sites and building costs.

6.1 Significance of results

The result shows an extreme scenario regarding the impact of large EV batteries on the decision-making of installing new charging stations and their impact on the electrical grid system. Increasing battery capacity, EV adaption rate, and the number of daily charging at a station shows how profitable charging stations can be in the future as society adjusts to climate change by phasing out internal-combustion engines. However, the case has two sides, rising battery capacity, EV adaption rate, and charging times create high loads in the grid system. Leading to an expansion of lines, transformers, generators, and storage units. Resulting in a high annual system cost for electricity producers. This shows the importance of modeling both cases since they are interconnected.

6.2 Comparison with prior work

Not all parameters are stated in the original musk-model in [23], making it hard to validate the results. The paper's main objective was to focus on the return on investment regarding the optimal location of EVs. The objective value is not stated throughout the paper, making it hard to validate whether the scenario modeled is profitable. The mathematical model can force installations of new charging stations since N is set to a fixed number, even when the profits are negative. Also, there is an inconsistency in the profit and cost variables in the objective function. The charging price at s station p is denoted in Sek/min, while the electricity cost for the charging at a station p_e is denoted in Sek/kWh. Ultimately, this cancels out in the objective function but results in only the charging price at a station being dependent on the charging time t of an EV. The electricity cost of charging an EV ultimately acts as a marginal price for which the price of charging should be higher. In reality, both would depend on the charging time t since the difference between the marginal price and the charging price at the station should determine the objective value. This is changed during the new implementation of the musk-model, making the charging time t not impact the objective function. Instead, the charging time is reflected in the number of servings a charger can have during a day m.

To solve the issue where the musk-model selects locations for charging stations with negative profits, the amount of charging stations to install is changed from a fixed variable to a decision variable. Making the model select the optimal number of new charging stations to maximize profits. The existing traffic flow determines the number of new charging stations and selects locations where existing charging stations do not already meet the demand.

A new constraint is introduced to more accurately tailor the model to the Norwegian market by implementing a governmental incentive, which is created to encourage station builders to install more rapid chargers for heavy-duty EVs. The incentive is modeled to cover 80 percent of the investment cost, reducing costs and raising profits from building new rapid charging stations. The upper bound of the total incentive is set not to exceed the limit of the total incentive distributed by the Norwegian government.

Sensitivity analysis was suggested as future research in the original paper upon which the musk-model was built. The sensitivity of several parameters in the modified musk-model shows how each parameter contributes to the model's profitability.

6.3 Model limitations

The musk-model is a user-friendly mathematical model. One of the biggest flaws is how the profits are modeled. It measures the daily profits for one year by subtracting the daily costs from the daily profits. This excludes profits during a charging station's lifetime and free cash flow generated by the investment. Instead, the profitability of the investment should be determined by the project's Net Present Value (NPV). It includes a more accurate framework for determining if a project is profitable. By setting the investment cost to be the costs for investing in long-term assets in year zero, it can be depreciated during the project's lifetime, reducing taxes. A discount rate can be selected to determine the investment's required minimum return. Inflation and operational costs (maintenance, salaries, etc) can be included annually, reducing the profits before taxes. The tax reduces the profits and results in the investment's free cash flow, which can be used to find the investment's net present value by a given discount rate, like the Weighted Average Cost of Capital (WACC). The model will select the projects with the highest NPV as the most profitable, while projects below zero are nonprofitable.

The original musk-model considered land-use classification in the decision-making for selecting optimal locations by giving each grid cell a value from 0-100 percent based on how much of the area in a cell contained the desired land-use class. Then the value is multiplied by the initial traffic flow v_0, diminishing demand v_i. During the data gathering for the musk-model, land-use classification data were not achieved due to the data not being intended for the public. It exists in Norway and can be found at [68]. However, other suggestions proposed using machine learning to classify different land-use classifications but were out of the scope of this thesis. In the end, land-use classification data was discarded. As a result, the model regards every grid cell as equally suitable ($A_i/A = 1$) for installing new charging stations. A positive consequence is that the demand more accurately satisfies the actual traffic flow in each grid cell. Conversely, the most suitable locations for EV users are discarded since the selection of charging station locations near malls, gas stations, or shops is not included in the model. The utilization of land-use classification is important in urban planning and zoning decisions to help planners find a balanced mix between residential, commercial, and public locations to help avoid traffic congestion.

The measurement of traffic flow has several flaws. Including arrival times of EVs, the measurement points count traffic in both directions, making it hard to evaluate which direction a vehicle is headed and the current SoC of an EV. The measurement point is not present on all roads, making it necessary to implement average values for grids where traffic flow data is missing. Leading to values that might be inaccurate for many grid cells.

PyPSA-eur is based on open-source data sets. And it can be hard to validate what some data sets represent. For instance, data sets containing loads are based on *ENTSO-E* power statistics, according to a report [69], which include the quantity of electrical power the utility company delivers to the end users within the analyzed network. This total net electricity is generated domestically or imported directly from foreign sources by industrial or commercial firms within the network, used for their own requirements or to serve end-users directly. Making it hard to know how many and which chargers are already included as loads. Some data are even based on Wikipedia articles, like line types. This creates an issue since the information can be changed in real-time, ultimately affecting the model results.

The model for analyzing the impacts of charging infrastructure in the grid system is currently limited to the full year of 2013, with snapshots of data such as loads and generation aggregated to 24 hours. In attempts to implement a cutout from ERA5 and Sarah-2 for 2018 to 2022, complications with other data sets occurred, causing several data in the model to be missing, but according to the authors of PyPSA-eur it should be fully possible to create models based on data from ERA5 and Sarah-2 from 1940 to present.

Currently, the model is automatically simplified and clustered into a selected number of nodes in Southern Norway. The analytical part is limited to Southern Norway since Northern Norway is represented as one single node in the model.

This makes it hard to analyze components in the grid at the region of interest. Instead, the existing charging infrastructure was added along with new ones to create enough load in the system to see an impact on the national grid. PyPSA-eur is a highly modifiable framework for which new features can be built, so it is not impossible to modify the simplification and clustering scripta *cluster_network.py* and *simplify_network* to the region of interest.

The model only consists of the overlying topology of the grid system, meaning lines with a voltage above 220 kV. In the simplification part of the model, the transmission network is mapped to a 380 kV voltage layer. Limiting the power system analysis to high voltage lines. Excluding the possibility of analyzing local lines below 220 kV. This would be highly valuable when analyzing the grid impacts of a selection of new chargers to the system.

6.4 Assumptions and reality

The objective function from the musk-model returned an immense daily profit of 608 092 NOK or 222 million NOK and a total revenue of 232 million per year, which means that they have net costs of 10 million (with incentives). The profit does not compare to what other companies are earning in today's market. Mer Norway AS has a total revenue of 252 million NOK and a negative 81 million NOK profit in 2022 [70]. The immense daily profits from the musk-model are not rooted in the model itself but in the assumptions made for the parameters m, v_0, and α. The serving times for each charger m are set to charge seven vehicles each day, which is the maximum serving times a charger can have with the given battery capacity α and the charger's output power. In addition, the battery capacity is modeled for heavy-duty EVs, which are further enhanced by the EV adaption rate v_0 being the same as today's adaption rate. In reality, the adaption rate is higher than possible for trucks to obtain. There are 68 407 registered trucks in Norway, meaning that the adaption rate of trucks can maximum represent under 6 percent of the total car fleet, never obtaining an adaption rate of 17.8 percent. Instead, the model represents the profits from giving the present EV fleet a battery capacity of 468 kWh, with every charger fully booked for the day. However, battery capacity and EV adaption are projected to rise based on growth over the last few years. This can be seen in the financial statement of Mer Norway AS, with an increase of roughly 600 percent in total revenue from 2018 to 2022.

Further, the costs are not accurately implemented in the musk-model. The balance sheet of Mer Norway AS [70] shows that the cost of goods is about 180 million, salaries 37 million, amortization 60 million, and other operational costs 56 million. However, the balance sheet looks better, with assets and equity increasing 250% and 670% in the last five years while the debt is decreasing. This could mean some costs are related to investing in new charging infrastructure.

The objective value from the model is instead showing how much potential EV charging can have as a business in the future. Despite having an unrealistically high objective value, the model still selects the most suitable locations based on where there is the most charging demand based on traffic flow, whether having high or low profits.

When the optimal locations of charging stations were selected, they were implemented in the power system as a load. The artificial time series represent an EV that drives 14 times weekly. It drives 200 km during a week and has a consumption of 0.18 kWh/km. This adds a weekly demand of 36 kWh to the power system. The same time series is implemented for every charger (26 599 chargers), resulting in an instantaneous need for the power system to deliver a total of 957 564 kWh to the vehicles weekly. This is not how EVs usually behave, but it is a valid scenario since there is a possibility that the EV fleet in Norway can occupy each charger and charge at the same time. The impact of the selected battery capacity of 468 kWh is not fully utilized. Still, it shows how sensitive the power system is to instantaneous charging demand and how expensive it is to enhance the grid based on the total annualized system cost.

The current model built in PyPSA-eur only includes the power grid of Norway. This is a simplification of how the power grid works in reality. The power grid connects across borders, and electricity is imported and exported based on whether demand within a country is high or low. This simplification causes the model to have a higher annualized total system cost since the country must produce all the electricity by itself.

7 Conclusion

7.1 Further research

To further enhance the musk-model future research should investigate how the traffic flow of heavy-duty EVs is distributed, by investigating the start and end of the route, to see where the traffic is coming from and better understand if heavy-duty EVs are traveling in limited areas where the model has built new charging stations. Further, investigate refined traffic flow data to get more useful insight into traffic patterns, adding the raw vehicle count and additional information about speed, vehicle type, and what times vehicles pass through the measurement point. Queuing theory could be implemented in the model to reduce congestion at stations since both heavy-duty EVs and EVs can charge at the same station. A better implementation of EV adaption rate, average battery capacity, and number of servings a day per charger should be implemented to more accurately model a real-world case, a suggestion could be to start with the EV adaption rate which heavy-duty EVs have today and then slowly upscale parameters by projecting the growth, to see which year charging of heavy-duty EVs could become profitable. A more accurate method for calculating profitability should be implemented to reflect better the time value of money and account for more costs, including salaries, taxes, yearly maintenance, and operations cost.

The power system model could be further enhanced by creating cutouts for several years to account for variations in weather by varying solar irradiation, wind speed, and temperature measurements to better project the generation from renewables like solar power and wind farms. During the thesis, PyPSA-eur was updated to include sector-coupling studies. Further investigation into this can be interesting since it can better project loads from different sectors, making it easier to analyze a more realistic scenario. A different implementation of the network components concerning battery and EVs can enhance the model to account for studies related to state-of-the-art technologies, like vehicle-to-grid. By implementing time series for which the vehicle is stationary and connected to the grid, renewable energy sources like wind and solar power can "get rid of" excess power by charging the batteries, which can be used as storage for when the demand is high and then discharged back into the power system when the loads are high, reducing the total system cost and prohibiting overloading in the power system.

7.2 Concluding remarks

The high daily profit evident in the musk-model highlights the future charging station's potential profitability. By optimally locating these stations, planners can establish a strong foundation for identifying the best sites for new chargers, especially where existing charging demand is unmet. Analyzing the sensitivity of various parameters can shed light on their impact on the musk-model's objective value. New additional constraints tailored for the Norwegian case study are implemented to model governmental incentives, leading to more charging sites for heavy-duty EVs. The integration with PyPSA-eur offers a robust open-source platform for assessing the impact of installations on the national power grid. It allows for examining how new loads might affect grid components, allowing planners to analyze lines, generators, storage units, buses, links, and loads. This insight is crucial for planners as new grid installations could change initial parameters in the musk-model and could result in having to reassess the model. The collaboration between the models offers an open-source tool for scholars, researchers, and planners to study the potential capacity of renovated or newly installed generators and the overall electricity generated from renewable sources. This analysis can reveal where new generators might be optimally placed to meet the rising demand from charging sites and construction costs and could be useful in models concerning state-of-the-art technologies.

Bibliography

[1] Statistics Norway. *11823: Registrerte kjøretøy, etter statistikkvariabel, drivstofftype og år*. https://www.ssb.no/statbank/table/11823/tableViewLayout1/. [Online; accessed 15-May-2023]. 2023.

[2] Statistics Norway. *08940: Klimagasser, etter kilde (aktivitet), energiprodukt, statistikkvariabel, år og komponent*. https://www.ssb.no/statbank/table/08940/tableViewLayout1/. [Online; accessed 15-May-2023]. 2022.

[3] Posten Norge AS. *Våre klima- og miljømål*. https://www.postennorge.no/baerekraft/klima-og-miljomal. [Online; accessed 15-May-2023]. 2023.

[4] Statnett. *Kortsiktig Markedsanalyse 2022-27*. https://www.statnett.no/globalassets/for-aktorer-i-kraftsystemet/planer-og-analyser/kma2022-2027.pdf. [Online; accessed 10-May-2023]. 2022.

[5] LKAB. *A faster pace and higher targets in LKAB's transition towards a sustainable future*. https://mb.cision.com/Main/11419/3553029/1568944.pdf. [Online; accessed 11-May-2023]. 2022.

[6] Statnett. *Brev til NVE om oppdatert investeringsplan 2022*. https://www.statnett.no/for-aktorer-i-kraftbransjen/planer-og-analyser/nettutviklings-og-investeringsplan/. [Online; accessed 15-May-2023]. 2022.

[7] Ole-Andre Isaksen. *Master Thesis - Optimal sizing and placement of Electrical Vehicle charging stations to serve Battery Electric Trucks*. [Online; accessed 25-May-2023]. May 2023. URL: https://github.com/o2i/Masters-Thesis.

[8] Masayuki Morimoto. "Which is the First Electric Vehicle?" In: *Electrical Engineering in Japan* 192.2 (2015), pp. 31–38. DOI: https://doi.org/10.1002/eej.22550. eprint: https://onlinelibrary.wiley.com/doi/pdf/10.1002/eej.22550. URL: https://onlinelibrary.wiley.com/doi/abs/10.1002/eej.22550.

[9] C. Sulzberger. "An early road warrior: electric vehicles in the early years of the automobile." In: *IEEE Power and Energy Magazine* 2.3 (2004), pp. 66–71. DOI: 10.1109/MPAE.2004.1293606.

[10] Hussain Shareef, Md. Mainul Islam, and Azah Mohamed. "A review of the stage-of-the-art charging technologies, placement methodologies, and impacts of electric vehicles." In: *Renewable and Sustainable Energy*

Reviews 64 (2016), pp. 403–420. ISSN: 1364-0321. DOI: https://doi.org/10.1016/j.rser.2016.06.033. URL: https://www.sciencedirect.com/science/article/pii/S1364032116302568.

[11] Rajanand Patnaik Narasipuram and Subbarao Mopidevi. "A technological overview design considerations for developing electric vehicle charging stations." In: *Journal of Energy Storage* 43 (2021), p. 103225. ISSN: 2352-152X. DOI: https://doi.org/10.1016/j.est.2021.103225. URL: https://www.sciencedirect.com/science/article/pii/S2352152X21009221.

[12] F. J. Soares et al. "State of the Art on Different Types of Electric Vehicles." In: *Electric Vehicle Integration into Modern Power Networks*. Ed. by Rodrigo Garcia-Valle and João A. Peças Lopes. New York, NY: Springer New York, 2013, pp. 1–13. ISBN: 978-1-4614-0134-6. DOI: 10.1007/978-1-4614-0134-6_1. URL: https://doi.org/10.1007/978-1-4614-0134-6_1.

[13] N. Hatziargyriou, E. L. Karfopoulos, and K. Tsatsakis. "The Impact of EV Charging on the System Demand." In: *Electric Vehicle Integration into Modern Power Networks*. Ed. by Rodrigo Garcia-Valle and João A. Peças Lopes. New York, NY: Springer New York, 2013, pp. 57–85. ISBN: 978-1-4614-0134-6. DOI: 10.1007/978-1-4614-0134-6_3. URL: https://doi.org/10.1007/978-1-4614-0134-6_3.

[14] Kwo Young et al. "Electric Vehicle Battery Technologies." In: *Electric Vehicle Integration into Modern Power Networks*. Ed. by Rodrigo Garcia-Valle and João A. Peças Lopes. New York, NY: Springer New York, 2013, pp. 15–56. ISBN: 978-1-4614-0134-6. DOI: 10.1007/978-1-4614-0134-6_2. URL: https://doi.org/10.1007/978-1-4614-0134-6_2.

[15] Abbas Fotouhi et al. "A review on electric vehicle battery modelling: From Lithium-ion toward Lithium–Sulphur." In: *Renewable and Sustainable Energy Reviews* 56 (2016), pp. 1008–1021. ISSN: 1364-0321. DOI: https://doi.org/10.1016/j.rser.2015.12.009. URL: https://www.sciencedirect.com/science/article/pii/S1364032115013921.

[16] Sergio Manzetti and Florin Mariasiu. "Electric vehicle battery technologies: From present state to future systems." In: *Renewable and Sustainable Energy Reviews* 51 (2015), pp. 1004–1012. ISSN: 1364-0321. DOI: https://doi.org/10.1016/j.rser.2015.07.010. URL: https://www.sciencedirect.com/science/article/pii/S1364032115006577.

[17] H. Paul Williams. *Model Building in Mathematical Programming, 5th Edition*. John Wiley & Sons Ltd, 2013.

[18] Zhile Yang, Kang Li, and Aoife Foley. "Computational scheduling methods for integrating plug-in electric vehicles with power systems: A review." In: *Renewable and Sustainable Energy Reviews* 51 (2015), pp. 396–416. ISSN: 1364-0321. DOI: https://doi.org/10.1016/j.rser.2015.06.007. URL: https://www.sciencedirect.com/science/article/pii/S1364032115005778.

[19] Derek Jackson, Yue Cao, and Ian Beil. “Bi-Level Optimization Framework for Heavy-Duty Electric Truck Charging Station Design.” In: *2022 IEEE Transportation Electrification Conference Expo (ITEC)*. 2022, pp. 563–568. DOI: 10.1109/ITEC53557.2022.9813815.

[20] Mouna Kchaou-Boujelben. “Charging station location problem: A comprehensive review on models and solution approaches.” In: *Transportation Research Part C: Emerging Technologies* 132 (2021), p. 103376. ISSN: 0968-090X. DOI: https://doi.org/10.1016/j.trc.2021.103376. URL: https://www.sciencedirect.com/science/article/pii/S0968090X21003776.

[21] Yutaka Motoaki. “Location-Allocation of Electric Vehicle Fast Chargers—Research and Practice.” In: *World Electric Vehicle Journal* 10.1 (2019). ISSN: 2032-6653. DOI: 10.3390/wevj10010012. URL: https://www.mdpi.com/2032-6653/10/1/12.

[22] Diego A. Giménez-Gaydou et al. “Optimal location of battery electric vehicle charging stations in urban areas: A new approach.” In: *International Journal of Sustainable Transportation* 10.5 (2016), pp. 393–405. DOI: 10.1080/15568318.2014.961620.

[23] Caiyun Bian et al. “Finding the optimal location for public charging stations – a GIS-based MILP approach.” In: *Energy Procedia* 158 (2019). Innovative Solutions for Energy Transitions, pp. 6582–6588. ISSN: 1876-6102. DOI: https://doi.org/10.1016/j.egypro.2019.01.071. URL: https://www.sciencedirect.com/science/article/pii/S1876610219300803.

[24] Sreten Davidov and Miloš Pantoš. “Planning of electric vehicle infrastructure based on charging reliability and quality of service.” In: *Energy* 118 (2017), pp. 1156–1167. ISSN: 0360-5442. DOI: https://doi.org/10.1016/j.energy.2016.10.142. URL: https://www.sciencedirect.com/science/article/pii/S0360544216315882.

[25] Kai Huang, Pavlos Kanaroglou, and Xiaozhou Zhang. “The design of electric vehicle charging network.” In: *Transportation Research Part D: Transport and Environment* 49 (2016), pp. 1–17. ISSN: 1361-9209. DOI: https://doi.org/10.1016/j.trd.2016.08.028. URL: https://www.sciencedirect.com/science/article/pii/S1361920915300778.

[26] Mehmet Erbaş et al. “Optimal siting of electric vehicle charging stations: A GIS-based fuzzy Multi-Criteria Decision Analysis.” In: *Energy* 163 (2018), pp. 1017–1031. ISSN: 0360-5442. DOI: https://doi.org/10.1016/j.energy.2018.08.140. URL: https://www.sciencedirect.com/science/article/pii/S0360544218316761.

[27] Thomas Brown, Jonas Hörsch, and David Schlachtberger. “PyPSA: Python for Power System Analysis.” In: *Journal of Open Research Software* 6.1 (2018), p. 4. DOI: 10.5334/jors.188. URL: https://doi.org/10.5334\%2Fjors.188.

[28] Ray Daniel Zimmerman, Carlos Edmundo Murillo-Sánchez, and Robert John Thomas. “MATPOWER: Steady-State Operations, Planning, and Analysis Tools for Power Systems Research and Education.” In: *IEEE*

Transactions on Power Systems 26.1 (2011), pp. 12–19. DOI: 10.1109/TPWRS.2010.2051168.

[29] Leon Thurner et al. "Pandapower - an Open Source Python Tool for Convenient Modeling, Analysis and Optimization of Electric Power Systems." In: *CoRR* abs/1709.06743 (2017). arXiv: 1709.06743. URL: http://arxiv.org/abs/1709.06743.

[30] F. Milano. "An open source power system analysis toolbox." In: *IEEE Transactions on Power Systems* 20.3 (2005), pp. 1199–1206. DOI: 10.1109/TPWRS.2005.851911.

[31] Richard Lincoln. *PYPOWER*. https://github.com/rwl/PYPOWER. [Online; accessed 28-April-2023]. 2023.

[32] Stefan Pfenninger and Bryn Pickering. "Calliope: a multi-scale energy systems modelling framework." In: *Journal of Open Source Software* 3.29 (2018), p. 825. DOI: 10.21105/joss.00825. URL: https://doi.org/10.21105/joss.00825.

[33] A. Greenhall, R. Christie, and J-P Watson. "Minpower: A power systems optimization toolkit." In: *2012 IEEE Power and Energy Society General Meeting*. 2012, pp. 1–6. DOI: 10.1109/PESGM.2012.6344667.

[34] Alberto J. Lamadrid et al. "Using the Matpower Optimal Scheduling Tool to Test Power System Operation Methodologies Under Uncertainty." In: *IEEE Transactions on Sustainable Energy* 10.3 (2019), pp. 1280–1289. DOI: 10.1109/TSTE.2018.2865454.

[35] Hilpert. S.; Günther. S.; Kaldemeyer. C.; Krien. U.; Plessmann. G.; Wiese. F.; Wingenbach. C. "Addressing Energy System Modelling Challenges: The Contribution of the Open Energy Modelling Framework (oemof)." In: (2017). DOI: 10.20944/preprints201702.0055.v1.

[36] Mark Howells et al. "OSeMOSYS: The Open Source Energy Modeling System: An introduction to its ethos, structure and development." In: *Energy Policy* 39.10 (2011). Sustainability of biofuels, pp. 5850–5870. ISSN: 0301-4215. DOI: https://doi.org/10.1016/j.enpol.2011.06.033. URL: https://www.sciencedirect.com/science/article/pii/S0301421511004897.

[37] Harald G. Svendsen and Ole Chr Spro. "PowerGAMA: A new simplified modelling approach for analyses of large interconnected power systems, applied to a 2030 Western Mediterranean case study." In: *Journal of Renewable and Sustainable Energy* 8.5 (Sept. 2016). 055501. ISSN: 1941-7012. DOI: 10.1063/1.4962415. eprint: https://pubs.aip.org/aip/jrse/article-pdf/doi/10.1063/1.4962415/13490752/055501_1_online.pdf. URL: https://doi.org/10.1063/1.4962415.

[38] Johannes Dorfner et al. *urbs: v0.6*. Version v0.6. Aug. 2016. DOI: 10.5281/zenodo.60484. URL: https://doi.org/10.5281/zenodo.60484.

[39] Jonas Hörsch et al. "PyPSA-Eur: An open optimisation model of the European transmission system." In: *Energy Strategy Reviews* 22 (2018),

pp. 207–215. DOI: 10.1016/j.esr.2018.08.012. URL: https://doi.org/10.1016\%2Fj.esr.2018.08.012.

[40] G. Lieberman F. Hillier. 11th Edition. McGraw Hill, 2021. ISBN: 1259872998.

[41] Fatima Dargam, Shaofeng Liu, and Rita A. Ribeiro. "On the Impact of Big Data Analytics in Decision-Making Processes." In: *EURO Working Group on DSS: A Tour of the DSS Developments Over the Last 30 Years*. Ed. by Jason Papathanasiou, Pascale Zaraté, and Jorge Freire de Sousa. Cham: Springer International Publishing, 2021, pp. 273–298. ISBN: 978-3-030-70377-6. DOI: 10.1007/978-3-030-70377-6_15. URL: https://doi.org/10.1007/978-3-030-70377-6_15.

[42] J.C. Nash. "The (Dantzig) simplex method for linear programming." In: *Computing in Science Engineering* 2.1 (2000), pp. 29–31. DOI: 10.1109/5992.814654.

[43] Pierre Borne et al. *Optimization in Engineering Sciences: Exact Methods*. eng. 11. Aufl. Automation - control and industrial engineering series. Somerset: Wiley-ISTE, 2013. ISBN: 9781848214323.

[44] Ralph E. Gomory. "Outline of an algorithm for integer solutions to linear programs." In: *Bull. Amer. Math. Soc. 64 (1958), 275-278* (1958). DOI: 10.1090/S0002-9904-1958-10224-4. URL: https://doi.org/10.1090/S0002-9904-1958-10224-4.

[45] Kurt Spielberg. "Enumerative Methods in Integer Programming." In: *Discrete Optimization II*. Ed. by P.L. Hammer, E.L. Johnson, and B.H. Korte. Vol. 5. Annals of Discrete Mathematics. Elsevier, 1979, pp. 139–183. DOI: https://doi.org/10.1016/S0167-5060(08)70347-9. URL: https://www.sciencedirect.com/science/article/pii/S0167506008703479.

[46] Franz Rothlauf. "Optimization Methods." In: *Design of Modern Heuristics: Principles and Application*. Berlin, Heidelberg: Springer Berlin Heidelberg, 2011, pp. 45–102. ISBN: 978-3-540-72962-4. DOI: 10.1007/978-3-540-72962-4_3. URL: https://doi.org/10.1007/978-3-540-72962-4_3.

[47] PyPSA Developers. *$PyPSA_eur$: ReadtheDocs*. https://pypsa-eur.readthedocs.io/en/latest/index.html. [Online; accessed 02-May-2023]. 2023.

[48] Xin-She Yang. "Chapter 1 - Introduction to Algorithms." In: *Nature-Inspired Optimization Algorithms*. Ed. by Xin-She Yang. Oxford: Elsevier, 2014, pp. 1–21. ISBN: 978-0-12-416743-8. DOI: https://doi.org/10.1016/B978-0-12-416743-8.00001-4. URL: https://www.sciencedirect.com/science/article/pii/B9780124167438000014.

[49] Patricia Ryser-Welch. "A Review of Hyper-Heuristics Framework." In: Apr. 2014.

[50] L. M. Ellwein et al. "Sensitivity Analysis and Model Assessment: Mathematical Models for Arterial Blood Flow and Blood Pressure." In: *Cardiovascular Engineering* 8 (2008), pp. 94–108. DOI: https://doi.org/10.1007/s10558-007-9047-3.

[51] Obed Sims. *Musk-Model*. [Online; accessed 15-May-2023]. July 2022. URL: https://github.com/obedsims/Musk-Model.

[52] Joshua Adam Taylor. *Convex Optimization of Power Systems*. Cambridge University Press, 2015. ISBN: 9781107076877. URL: https://www.cambridge.org/no/academic/subjects/engineering/control-systems-and-optimization/convex-optimization-power-systems?format=HB&isbn=9781107076877.

[53] PyPSA Developers. *PyPSA Read the Docs: components*. https://pypsa.readthedocs.io/en/latest/components.html. [Online; accessed 02-May-2023]. 2023.

[54] Fabian Neumann. *Course in: "Data Science for Energy System Modelling"*. https://fneum.github.io/data-science-for-esm/09-workshop-pypsa.html. [Online; accessed 02-May-2023]. 2023.

[55] Google Groups. *Your experience with solving time, computation power, cloud computing*. https://groups.google.com/g/pypsa/c/X27EAUNXLQE/m/-tJ8iKlOBAAJ. [Online; accessed 02-May-2023]. 2023.

[56] PyPSA Developers. *PyPSA-Eur: A Sector-Coupled Open Optimisation Model of the European Energy System*. https://github.com/PyPSA/pypsa-eur. [Online; accessed 02-May-2023]. 2023.

[57] Songrit Maneewongvatana and David M. Mount. "Analysis of approximate nearest neighbor searching with clustered point sets." In: *CoRR* cs.CG/9901013 (1999). URL: https://arxiv.org/abs/cs/9901013.

[58] The SciPy community. *scipy.spatial.KDTree*. https://docs.scipy.org/doc/scipy/reference/generated/scipy.spatial.KDTree.html. [Online; accessed 14-May-2023]. 2022.

[59] Argis Pro. *Calculate Geometry Attributes (Data Management)*. https://pro.arcgis.com/en/pro-app/latest/tool-reference/data-management/calculate-geometry-attributes.htm. [Online; accessed 15-May-2023]. 2023.

[60] Argis Pro. *Spartial Join*. https://pro.arcgis.com/en/pro-app/latest/tool-reference/analysis/spatial-join.htm. [Online; accessed 15-May-2023]. 2023.

[61] Argis Pro. *Fill Missing Values (Space Time Pattern Mining)*. https://pro.arcgis.com/en/pro-app/latest/tool-reference/space-time-pattern-mining/fillmissingvalues.htm. [Online; accessed 20-May-2023]. 2023.

[62] Norwegian Ministry of Transport. *National charging strategy*. https://www.regjeringen.no/contentassets/26d4c472862342b69e8d49803b45c36a/en-gb/pdfs/national-charging-strategy.pdf. [Online; accessed 15-May-2023]. Jan. 2023.

[63] Scania. *Rigid Truck Specifications*. https://www.scania.com/uk/en/home/products/trucks/battery-electric-truck.html. [Online; accessed 15-May-2023]. 2023.

[64] Andreas Schroeder and Thure Traber. "The economics of fast charging infrastructure for electric vehicles." In: *Energy Policy* 43 (2012), pp. 136–144. ISSN: 0301-4215. DOI: https://doi.org/10.1016/j.enpol.2011.12.041. URL: https://www.sciencedirect.com/science/article/pii/S0301421511010470.

[65] Statistics Norway. *Registered vehicles*. https://www.ssb.no/en/transport-og-reiseliv/landtransport/statistikk/bilparken. [Online; accessed 15-May-2023]. 2022.

[66] Statistics Norway. *09387: Electricity price, grid rent and taxes for households, by contents and quarter*. https://www.ssb.no/en/statbank/table/09387/chartViewLine/. [Online; accessed 15-May-2023]. 2020-2022.

[67] ENOVA SF. *Årsrapport 2022*. https://2022.enova.no/. [Online; accessed 14-May-2023]. 2023.

[68] Statistisk Sentralbyrå. *Arealbruk 2022*. https://kartkatalog.geonorge.no/metadata/arealbruk-2022/a965a979-c12a-4b26-90a0-f09de47dbecd. [Online; accessed 27-May-2023]. 2023.

[69] entsoe. *Load and consumption data: Specificities of member countries*. https://eepublicdownloads.entsoe.eu/clean-documents/pre2015/publications/ce/Load_and_Consumption_Data.pdf. [Online; accessed 27-May-2023]. 2023.

[70] Proff.no. *Mer Norway AS*. https://www.proff.no/regnskap/mer-norway-as/kristiansand-s/bensinstasjoner/IGG9CJK003X/. [Online; accessed 27-May-2023]. 2023.